

EVIDENCE OF MAGMATIC CASSITERITE MINERALIZATION AT THE NONG SUA APLITE-PEGMATITE COMPLEX, THAILAND

ROBERT L. LINNEN¹, ANTHONY E. WILLIAMS-JONES AND ROBERT F. MARTIN

Department of Geological Sciences, McGill University, 3450 University Street, Montreal, Quebec H3A 2A7

ABSTRACT

The Nong Sua intrusive complex, in peninsular Thailand, is a boron-rich, rhythmically layered aplite-pegmatite body that hosts Sn-W mineralization. Aplites and fine-grained pegmatite layers have granitic compositions, whereas coarse-grained plagioclase-tourmaline-rich and K-feldspar-rich pegmatite layers have compositions that trend away from, and toward the Or apex, respectively, in the system Q-Ab-Or-H₂O. Whole-rock concentrations of tin in nonmineralized aplite and pegmatite correlate positively with K-feldspar abundances and are inversely proportional to primary muscovite and tourmaline contents. These relationships suggest that K-feldspar crystallization was relatively late, which is also supported by textural data, and that tin behaved as an incompatible element during the evolution of the magma. Nonmineralized K-feldspar-rich pegmatite contains up to 42 ppm Sn and, using the available mineral-melt partition coefficients, is estimated to have been in equilibrium with a melt that contained on the order of 700 ppm Sn. This value is close to experimentally determined levels of saturation for cassiterite in granitic melts. With further crystallization or changes of intensive parameters, such as an increase of $f(O_2)$, cassiterite crystallized directly from the pegmatite-forming melt. The onset of cassiterite crystallization is estimated to have occurred at approximately 95% crystallization, calculated by Rayleigh fractionation. Cassiterite disseminated in pegmatite has planar or embayed contacts with plagioclase and myrmekite (both An₅ to An₁₃) and perthite, and feldspars at embayed contacts contain inclusions of cassiterite. These textures suggest that cassiterite crystallized at, or prior to, vapor saturation. Irrespective of the timing of vapor saturation, the orthomagmatic fluid had a low salinity; in light of vapor-melt partition data, at least some of the cassiterite must have crystallized from melt. Vapor saturation also gave rise to cassiterite and wolframite mineralization hosted by quartz-tourmaline veins in aplite that terminate abruptly at aplite-pegmatite contacts. The latter relationship suggests that the hydrothermal mineralization also formed while the pegmatite was above solidus conditions. The presence of residual disorder in the feldspars and the persistence of oligoclase indicate that this aplite-pegmatite complex did not undergo protracted fluid-mediated recrystallization.

Keywords: aplite, pegmatite, petrogenesis, tin, tungsten, cassiterite, mineralogy, feldspar, geochemistry, Thailand.

SOMMAIRE

Le complexe intrusif de Nong Sua, en Thaïlande péninsulaire, contient des niveaux rythmiquement interlités d'aplite et de pegmatite borifères et une minéralisation en Sn et W. Les niveaux aplitiques et pegmatitiques à granulométrie fine possèdent une composition granitique, tandis que les niveaux pegmatitiques à granulométrie plus grossière, enrichis en plagioclase + tourmaline ou en feldspath potassique, ont des compositions qui s'éloignent et se rapprochent, respectivement, du pôle Or dans le système Q-Ab-Or-H₂O. La concentration en étain des échantillons d'aplite non minéralisés et de pegmatite montrent une corrélation positive avec la proportion de feldspath potassique, et négative avec la teneur en muscovite primaire et en tourmaline. Ces relations font penser que la cristallisation du feldspath potassique a été relativement tardive, comme l'indiquent les textures, et que l'étain s'est comporté comme élément incompatible au cours de l'évolution du magma. La pegmatite non minéralisée riche en feldspath potassique contient jusqu'à 42 ppm de Sn; d'après les coefficients de partage disponibles entre minéraux et liquide silicaté, le magma en équilibre avec une telle roche en contiendrait de l'ordre de 700 ppm. Cette valeur est proche des niveaux de saturation de la cassitérite dans un liquide granitique, tels que déterminés expérimentalement. Au cours de la cristallisation, ou avec un changement dans les paramètres intensifs, une augmentation en $f(O_2)$, par exemple, la cassitérite a cristallisé directement du magma qui a produit les pegmatites, après 95% de cristallisation, selon le modèle de fractionnement de Rayleigh. La cassitérite disséminée dans la pegmatite montre des contacts à aspect planaire ou "corrodé" avec le plagioclase et la myrmékite (An₅ à An₁₂ dans les deux cas) et la perthite, et les deux feldspaths contiennent des inclusions de cassitérite près des contacts à aspect "corrodé". Ces textures font penser que la cassitérite a cristallisé avant ou au cours de la saturation du magma en phase volatile. Quel que soit le point de saturation en phase volatile, le fluide orthomagmatique était de faible salinité; à la lumière des données sur le partage de l'étain entre phase volatile et magma, au moins une partie de la cassitérite a dû cristalliser à partir du magma. La saturation en phase volatile a aussi donné lieu à la formation de cassitérite et de wolframite dans des veines à quartz + tourmaline dans l'aplite; celles-ci sont abruptement terminées aux contacts entre aplite et pegmatite. Le stade hydrothermal de la minéralisation se serait donc formé quand la pegmatite se trouvait toujours au dessus du solidus. La présence de désordre résiduel dans les feldspaths et la persistance de l'oligoclase montrent que ce complexe d'aplités et de pegmatites a refroidi sans recristallisation poussée par interaction prolongée avec la phase fluide.

(Traduit par la Rédaction)

Mots-clés: aplite, pegmatite, pétrogenèse, étain, tungstène, cassitérite, minéralogie, feldspath, géochimie, Thaïlande.

¹Present address: C.R.S.C.M. - C.N.R.S., 1A, rue de la Férollerie, 45071 Orléans Cedex 2, France.

INTRODUCTION

Although tin mineralization is typically associated with granitic rocks, the occurrence of cassiterite as a magmatic mineral has generally been viewed with caution (*cf.* Taylor 1979). Such caution appears to have been justified by experimental data, summarized by Štemprok (1990), which show that tin is relatively soluble in granitic melts. This led Štemprok (1990) to suggest that the degree of fractionation required to achieve saturation in cassiterite in a natural granitic melt is unlikely to occur. However, the solubility of tin in granitic melts is a complex function of a variety of parameters, including T , $f(\text{O}_2)$, K/Na ratio, alkali:aluminum ratio, and the composition of the coexisting aqueous fluid (Taylor 1988, Taylor & Wall 1992). The possibility that the magma will become saturated in cassiterite is particularly enhanced if a low-salinity aqueous fluid is exsolved (Taylor & Wall 1992). Thus cassiterite in some environments may, in fact, be primary. In peninsular Thailand, cassiterite mineralization is commonly hosted by boron-rich granitic pegmatites (Charusiri 1989), and some authors have linked the mineralization in these pegmatites to magmatic processes. For example, Manning (1986) suggested that the cassiterite may have crystallized from an orthomagmatic fluid. However, there has been no systematic investigation of the genesis of tin mineralization in Thailand, and the possibility that some of this mineralization may be magmatic remains untested. The object of this paper is to report the results of a study of the unusually fresh aplite-pegmatite complex at Nong Sua, which hosts cassiterite and wolframite mineralization. Geological and petrographic relationships and observed assemblages of minerals at this deposit indicate that some cassiterite could have formed at magmatic conditions. This hypothesis is tested using major- and trace-element data, together with mineral-melt and fluid-melt partition calculations, and evidence is presented that direct magmatic crystallization of cassiterite is a predictable consequence of the evolution of the magma.

REGIONAL GEOLOGY

The Nong Sua tin-tungsten deposit is hosted by a rhythmically layered pegmatite-aplite complex located 10 km west of Prachuab Khiri Khan, approximately 180 km south of Bangkok (Fig. 1). The aplite-pegmatite forms a small hill surrounded by a plain of Quaternary sediments. Biotite granite, which forms part of the Cretaceous-Tertiary western Thai granite belt, outcrops less than 5 km west of Nong Sua (*cf.* Cobbing *et al.* 1986), and exposures of metamorphosed pebbly mudstone and

sandstone of the Carboniferous to Permian Kaeng Krachan Group occur at roughly the same distance north of Nong Sua (Fig. 1). Minor hornblende granite also is exposed 10 to 15 km southwest of Nong Sua, but its relationship to the biotite granite has not been established. The Kaeng Krachan Group adjacent to the western Thai granite belt in the Nong Sua area has been metamorphosed to the biotite facies, and the grade of metamorphism decreases away from the granites to subgreenschist facies near the Kaeng Krachan dam. A muscovite sample from the Nong Sua pegmatite yielded a total fusion $^{40}\text{Ar}/^{39}\text{Ar}$ date of 63.9 ± 0.6 Ma, and an $^{40}\text{Ar}/^{39}\text{Ar}$ plateau age of 53.2 ± 0.7 Ma was determined for biotite separated from a biotite granite located approximately 35 km southwest of Nong Sua (Fig. 1; Charusiri 1989). Whether the pegmatite is truly older than the biotite granite is beyond the scope of this study. However, the gross similarity of the ages indicates that the Nong Sua aplite-pegmatite and the biotite granite both belong to the western Thai granite province, but the age difference underlines the fact that the relationships between granite and pegmatite are poorly constrained.

GEOLOGICAL SETTING

The Nong Sua complex consists of alternating and laterally continuous horizons of pegmatite, aplite and metasedimentary rocks (Fig. 2). Aplites are weakly layered to massive and, on the basis of minerals present, are divided into garnet- and tourmaline-bearing aplite units. Much of the pegmatite is strongly layered and thus has been designated banded pegmatite. A second pegmatitic unit forms massive tourmaline-rich layers that are conformable to layering in the banded pegmatite, and this unit has been designated tourmaline pegmatite. The attitude of the layering in the aplite and pegmatite is consistent, with a strike of $215^\circ \pm 10^\circ$ and a dip of $35^\circ \pm 5^\circ$ to the northwest. Owing to the shallow dip of the aplite-pegmatite, the plan view is of limited use in showing the distribution of the different units. Nine vertical sections were therefore measured along the length of the complex, and a longitudinal section was constructed to show this distribution (Fig. 2).

APLITES

The garnet and tourmaline aplites are distinguished by the respective presence or absence of garnet. Both units are generally massive, but contain minor pegmatite horizons less than 10 cm thick that impart a weak layering to the rock. The lateral continuity of individual layers of aplite ranges up to 100 m along strike (Fig. 2), and the

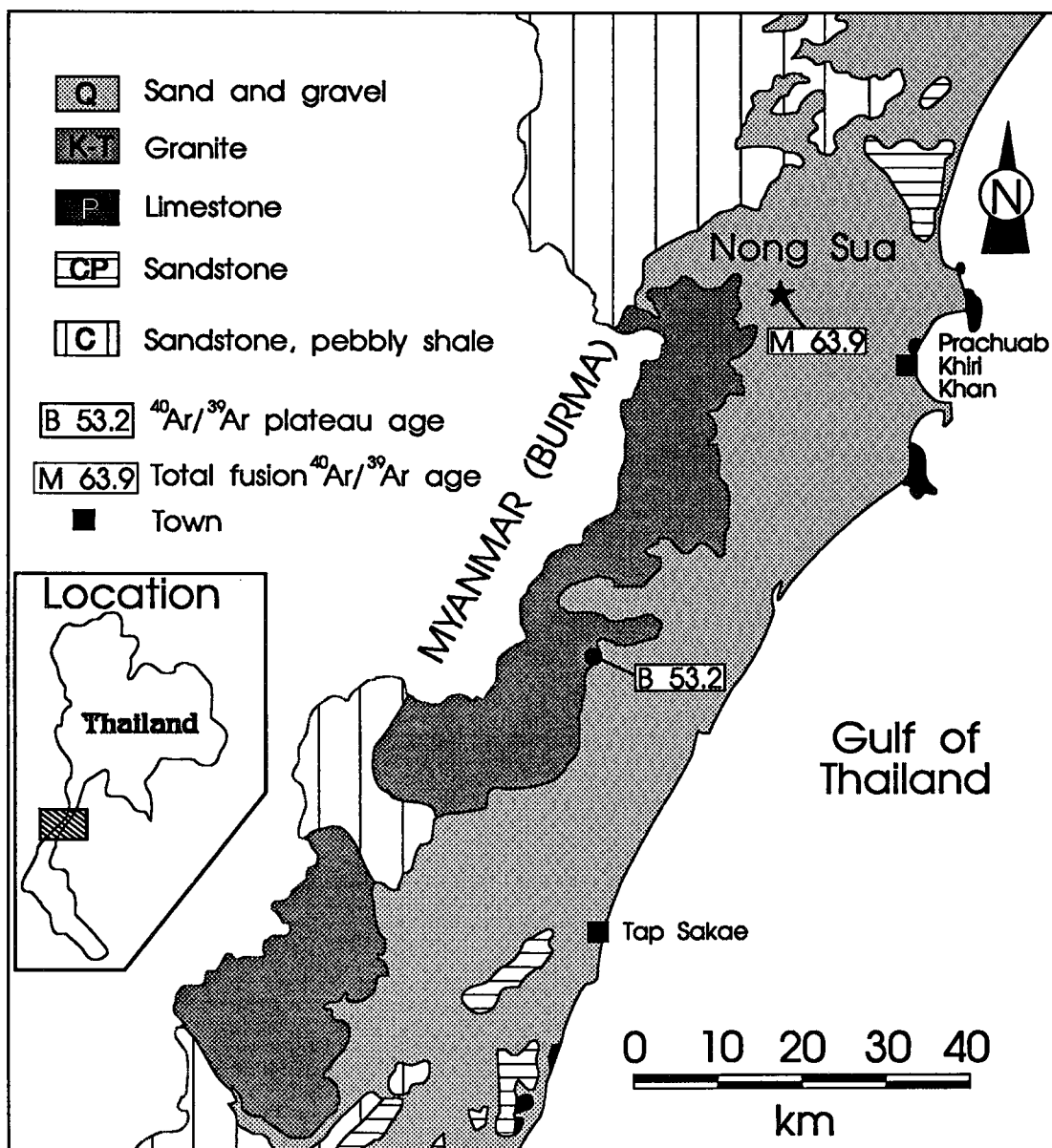


FIG. 1. Geology of the Prachuab Khiri Khan area, modified after Silpalit *et al.* (1985). $^{40}\text{Ar}/^{39}\text{Ar}$ ages of muscovite (M) and biotite (B) are from Charusiri (1989).

contacts between aplites and pegmatites are very sharp and parallel to layering in the pegmatite. A complete lack of contact irregularities, such as embayments or inclusions of one unit in another, suggests that both aplites and pegmatite crystallized from a single batch of magma.

The aplites are composed of quartz, K-feldspar

and plagioclase \pm muscovite \pm tourmaline \pm garnet \pm apatite. The grain size is variable, typically <0.5 to 2 mm, with some larger anhedral grains of K-feldspar up to 2 cm across. Garnet forms equant subhedral grains that are locally concentrated in laminae parallel to, or at a shallow angle to, the principal layering. More commonly,

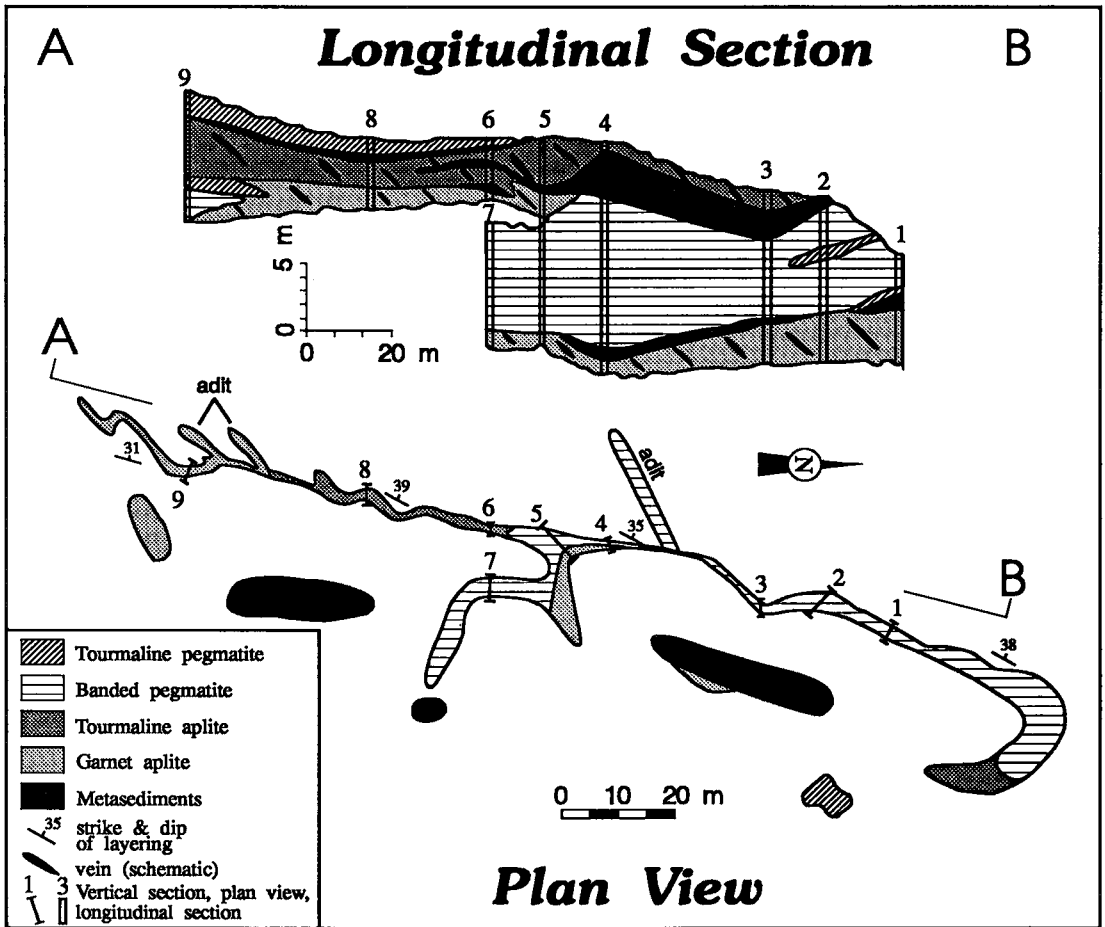


FIG. 2. A plan view and longitudinal section showing the geology of the Nong Sua apatite-pegmatite complex.

garnet is disseminated as clusters, up to 0.5 cm across, of anhedral grains. Tourmaline is present as disseminated grains up to 5 mm across that are typically subhedral and poikilitic, with inclusions of anhedral quartz.

Primary plagioclase generally occurs as subhedral to euhedral grains in sharp contact with all other phases; its composition (determined by electron-microprobe analysis) typically ranges from An_5 to An_{13} (Fig. 3). Plagioclase is typically white or cream-colored; locally, some coarse grains are grey, and more translucent. Myrmekite contains plagioclase that is compositionally similar to primary plagioclase and is locally observed as a replacement of K-feldspar, but myrmekite is much more widespread in pegmatite. The significance of this will be discussed below. Plagioclase also is

found as exsolved lamellae, as inclusions, and as discontinuous veinlets in perthite, generally with a composition of An_0 to An_3 .

K-feldspar is anhedral, in contrast to plagioclase. Coarse-grained perthite crystals are irregularly distributed in a fine-grained matrix composed mainly of plagioclase, quartz and microcline. K-feldspar is commonly white, but the occurrence of coarse-grained, grey, translucent K-feldspar is more widespread than that of grey plagioclase. The presence of euhedral crystals of plagioclase that extend from the matrix into the perthite (Fig. 4a) suggests that the crystallization of K-feldspar postdated much of that of plagioclase; this is supported by the presence of euhedral plagioclase inclusions in K-feldspar. Fine-grained K-feldspar is commonly present as cross-hatched twinned

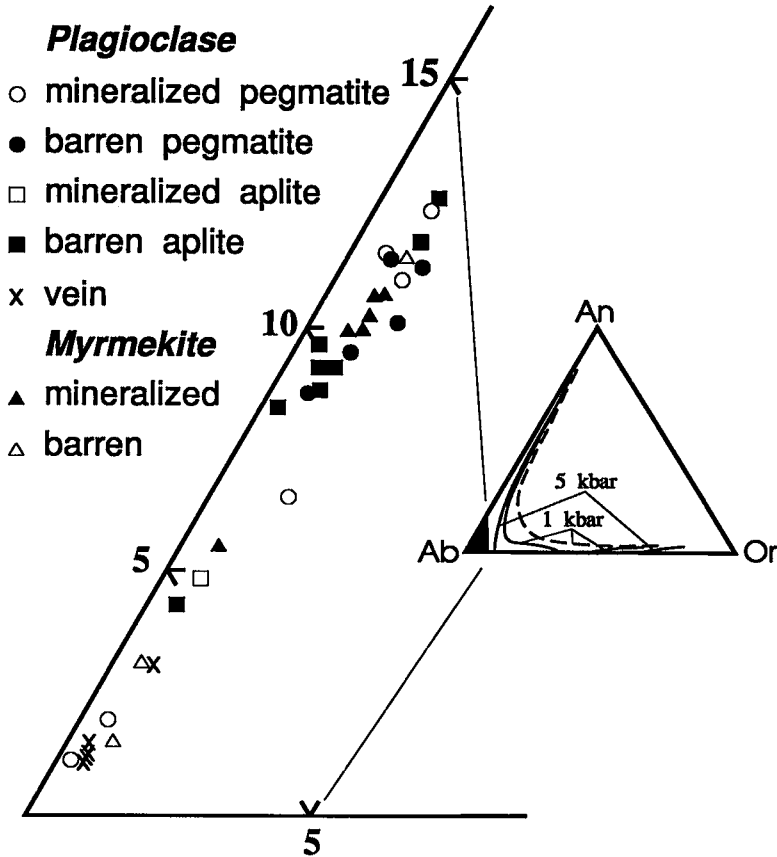


FIG. 3. Plagioclase and myrmekite compositions from barren and mineralized aplite and pegmatite and from mineralized veins. Each point represents the average composition determined by electron-microprobe analysis of several crystals in a single sample. The field of Nong Sua plagioclase compositions (shaded black) and the 650° (solid lines) and 750°C (dashed line) feldspar compositions at 1 and 5 kbar from Seck (1971) are shown on the offset Ab-An-Or diagram.

microcline in the groundmass, without visible perthite exsolution. The origin of the fine-grained K-feldspar is uncertain; however, its interstitial nature may indicate that it also is late in the paragenetic sequence. The Or content of the K-feldspar portion of perthite and of the fine-grained microcline (determined by electron microprobe analysis) generally ranges from 0.90 to 0.96, although the most sodic compositions may reflect sampling of Ab-rich domains (see section on details of feldspar mineralogy, below). Quartz and K-feldspar, and rarely quartz and plagioclase, are present as dendritic micrographic intergrowths but, like myrmekite, these textures are much more common in pegmatite and are discussed below.

Undulose extinction in quartz and feldspars, and fractured garnet and tourmaline crystals, are locally observed in aplite, similar to the deformation-induced features observed in pegmatite, discussed below.

PEGMATITE

The pegmatite units are distinguished texturally; the tourmaline pegmatite is massive, whereas the banded pegmatite is strongly layered. However, it should be noted that only tourmaline pegmatite layers greater than 2 m thick are represented on Figure 2; there are additional layers of tourmaline pegmatite within the banded pegmatite unit that

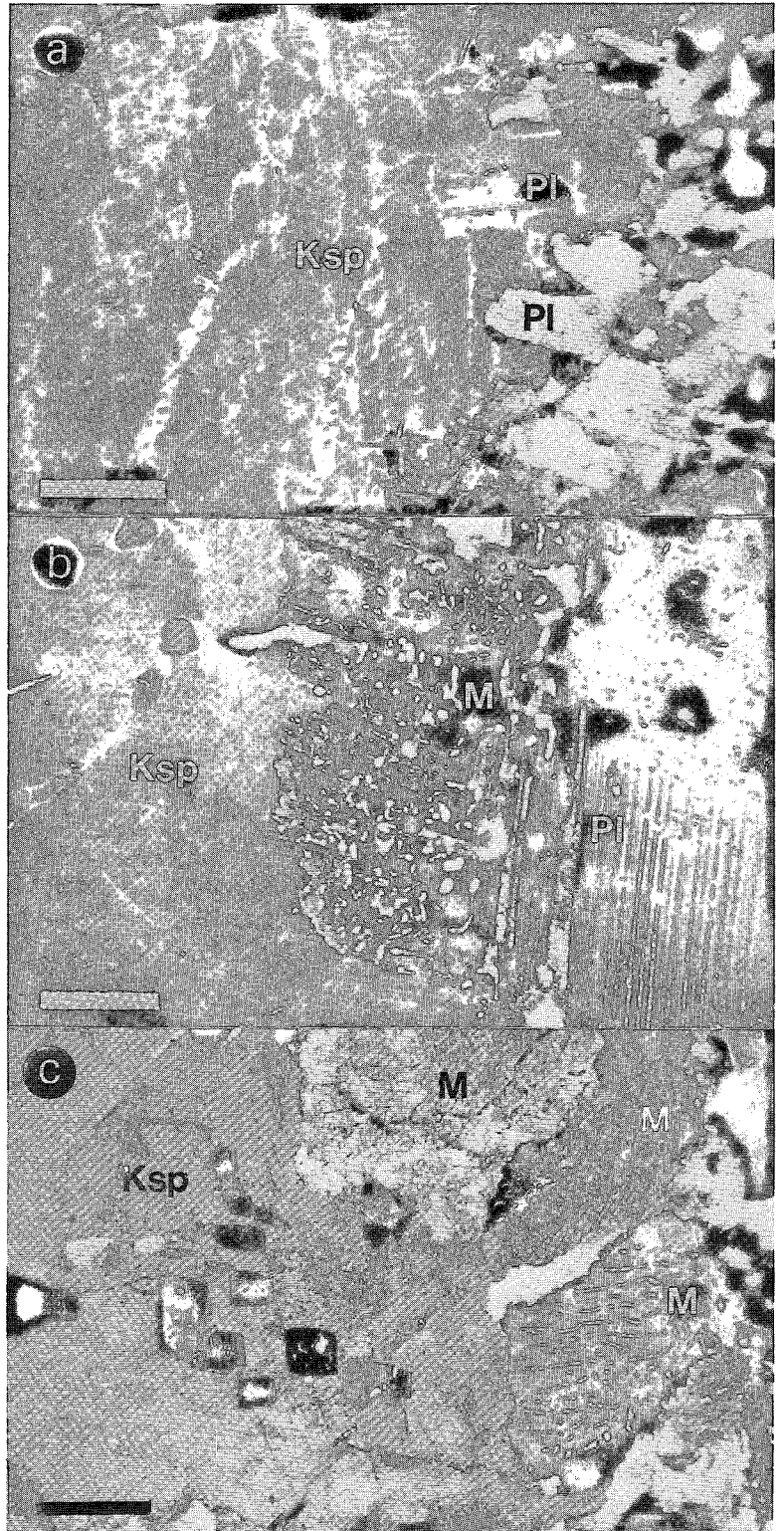


FIG. 4. Photomicrographs of feldspar textures. a) Euhedral plagioclase (Pl) enclosed by coarse-grained anhedral perthite (Ksp). Some cross-hatched twins, related to undulose extinction, are visible in the upper left-hand corner. The bar scale represents 0.5 mm. b) Bulbous myrmekite (M) between K-feldspar (Ksp) and plagioclase (Pl). Albite twins are destroyed in the myrmekite domain. The bar scale represents 0.5 mm. c) Graphic-like myrmekite (M) replacement of K-feldspar. The bar scale represents 0.5 mm.

are too thin to be represented at this scale. Both units are composed of quartz, plagioclase, K-feldspar, tourmaline, muscovite, and trace apatite; minor garnet is locally present in the banded pegmatite. Layering in the banded pegmatite is recognized by changes in grain size, changes in the modal proportions of minerals, or both. Variation in the local abundance of tourmaline helps define light and dark horizons in which tourmaline or feldspar crystals are commonly in sharp contact with other primary minerals, and are oriented perpendicular to the layering. These features are interpreted to reflect a magmatic origin for the layering.

The banded pegmatite consists of the following five lithologies and gradations between them: 1) fine-grained tourmaline-rich pegmatite, 2) fine-grained aplite, 3) coarse-grained K-feldspar-rich pegmatite, 4) coarse-grained graphic quartz - K-feldspar pegmatite, and 5) coarse-grained tourmaline-rich pegmatite. Thin (<10 cm) quartz - K-feldspar - plagioclase - tourmaline \pm muscovite dykes also cross-cut the pegmatite and aplite units locally. The grain size of the banded pegmatite varies from 2 to 5 mm in the fine-grained tourmaline-rich pegmatite and aplite layers to greater than 10 cm in the coarse-grained K-feldspar-rich and graphic pegmatite layers. The coarse-grained tourmaline-rich pegmatite typically contains crystals 2 to 5 cm (rarely up to 15 cm) long. Fine-grained tourmaline-rich layers are volumetrically the most important lithology in the banded pegmatite. They are composed of coarse-grained anhedral perthite (up to 5 cm across) set in a finer-grained matrix of plagioclase, quartz, tourmaline, muscovite and K-feldspar (locally containing visible exsolved perthite and cross-hatched twins).

The ratio of K-feldspar to plagioclase in the different units of banded pegmatite is highly variable, but much of the fine-grained tourmaline-rich unit has a granitic composition (discussed below). Coarse-grained tourmaline-rich pegmatite typically contains very little K-feldspar, but subhedral to euhedral primary muscovite grains up to 3 cm across are common. K-feldspar-rich pegmatite is composed of either graphic quartz-perthite intergrowths, best developed immediately above the garnet aplite contact (near section 7, Fig. 2), or perthite-quartz layers in which K-feldspar crystals are euhedral. A trace of metasomatic K-feldspar occurs along fractures in plagioclase, but there is no petrographic evidence that suggests widespread potassic or sodic metasomatism. Both white and grey varieties of plagioclase and K-feldspar are present in pegmatite, and as in the case for the aplites, grey translucent feldspars are typically coarse-grained, and grey K-feldspar is more

common than grey plagioclase. The importance of the variation in color is discussed below.

A significant proportion of the perthite, including that in graphic quartz-perthite intergrowths, has been converted to microcline. Domains of cross-hatched twinning are spatially associated with zones of undulose extinction and are therefore considered to have been stress-induced. A similar association between visible exsolution lamellae in perthite and undulose extinction may indicate that coarsening of exsolved albite also was stress-related. Most of the K-feldspar in perthite and cross-hatched twinned microcline have compositions ranging from Or₉₀ to Or₉₆ and contain a negligible anorthite component, *i.e.* they are compositionally similar to aplite-hosted perthite. As in that case, and in view of compositions derived from X-ray-diffraction data (see below), the sodic end of this range is due to sampling of albite domains by the electron beam during analysis.

Plagioclase, which displays primary textures, generally has a composition ranging from An₁₅ to An₁₃; within most crystals and amongst crystals in the same sample, the variation is less than An₁ (also the case in aplite). The Or content is typically <2% (Fig. 3). A comparison of the plagioclase compositions with those on the 650° and 750°C solvi of Seck (1971) in Figure 3 indicates that the plagioclase has undergone re-equilibration (loss of potassium to a fluid phase). This is not surprising since re-equilibration of feldspars is a pervasive feature in granitic rocks (*cf.* Parsons & Brown 1984).

A conspicuous feature of the pegmatites and, to a lesser extent, the aplites, is the occurrence of myrmekite at perthite-plagioclase grain boundaries. Myrmekite generally forms anhedral masses that separate the subhedral to euhedral plagioclase from perthite. The myrmekite forms part of the plagioclase crystal, and albite twins, visible elsewhere in the plagioclase, are commonly destroyed in the domain occupied by the myrmekite. Myrmekite contacts are convex into the perthite and are bulbous or lobate (Fig. 4b; *cf.* Phillips 1974, Hibbard 1979). These textures suggest that the myrmekite represents the product of a reaction between perthite and plagioclase. Less commonly, myrmekite contacts are irregular, with numerous re-entrants in perthite, or myrmekite zones cross-cut single grains of perthite. These features support a replacement origin for the myrmekite.

The plagioclase in myrmekite generally is compositionally indistinguishable from non-myrmekitic plagioclase in the same sample. In both cases, there is a lack of compositional zonation, and the An contents are 5 to 13 mol%, depending on the sample (Fig. 3). Some myrmekite grains are zoned, being most sodic at K-feldspar contacts; the most calcic myrmekite has the same An-Ab-Or

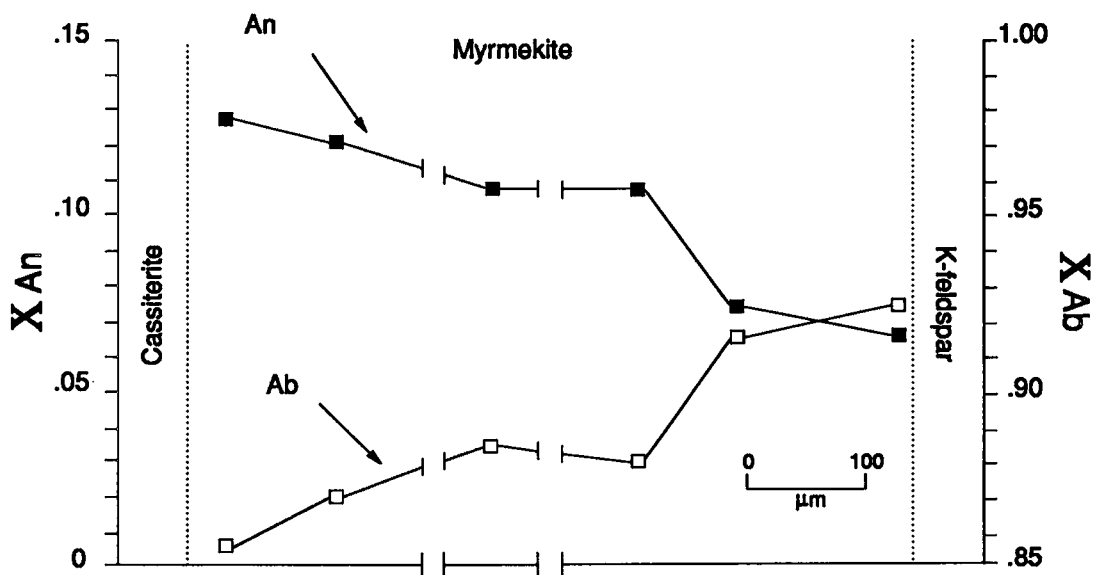


FIG. 5. Plagioclase compositions along the zoned myrmekite grain on Figure 7b; the dotted lines represent the locations of the embayed contacts with cassiterite and perthite.

proportions as non-myrmekitic plagioclase in the same sample. An example of this zoning is illustrated in Figure 5. Finally, the myrmekite at Nong Sua is unusual in that the "wormy quartz" is more commonly rod-shaped, and the quartz rods within myrmekite grains are optically continuous (Fig. 4c); hence, the myrmekite is texturally transitional to graphic quartz-plagioclase, but is here considered as myrmekite, because it is invariably related to replacement of K-feldspar.

True graphic intergrowths are much less common than myrmekite, and are developed mainly between quartz and perthite. Rare graphic intergrowths of plagioclase and quartz are observed in aplite. These grains have a plumose structure, with optically continuous quartz radiating outward. Perthite that is graphically intergrown with quartz is otherwise indistinguishable from that described above. It may contain plagioclase inclusions and is commonly rimmed by plagioclase and myrmekite. In some cases, the rods of graphic quartz intergrown with perthite extend into the myrmekite, indicating that the latter replaced pre-existing perthite.

Deformation features are variably developed in the pegmatite. These include: 1) crystals of tourmaline broken perpendicular to the *c* axis, 2) kinked muscovite, 3) quartz, plagioclase and K-feldspar with undulose extinction, and 4) plagioclase with displaced twins. Quartz and

feldspar are unstrained in some samples, and highly deformed in others.

METASEDIMENTARY ROCKS

Tabular blocks of massive metasandstone of the Kaeng Krachan Group composed of quartz, biotite, muscovite, plagioclase, rutile and, locally, hornblende, are contained within the aplite-pegmatite complex (Fig. 2). The blocks are oriented parallel or subparallel to layering in the pegmatite; pegmatite dykes rarely cross-cut individual metasedimentary blocks. Paucity of outcrop precludes the establishment of the aplite-pegmatite as a large dyke cutting the Kaeng Krachan Group or of the blocks of metasedimentary rocks as roof pendants. Within 10 cm of aplite or pegmatite, the metasandstone is generally altered to a tourmaline-quartz assemblage.

MINERALIZATION

Three modes of mineralization are recognized at the Nong Sua deposit and these have been distinguished as vein, disseminated and greisen styles. Cassiterite is present in all the styles, whereas wolframite is almost exclusively vein-hosted. Disseminated cassiterite also contains significant concentrations of Ti-Nb-Ta oxide minerals. The timing of each style of mineralization is constrained by textural and structural relationships with the

host aplite and pegmatite, and thus the crystallization of cassiterite and wolframite can be related to the evolution of the pegmatitic system. The relative economic importance of the different styles of mineralization cannot be ascertained, as the mine is not currently in production, and records of past production are not available.

Vein mineralization

Mineralized veins are hosted by aplite; they are discordant to layering, less than 1 m thick, less than 10 m long, and generally lack alteration haloes. Contacts between veins and aplite are usually very sharp, with the mineralization being restricted to the vein. Rarely, vein contacts are diffuse, and quartz has replaced feldspars in the aplite. At such contacts, the mineralization may be disseminated in the wallrock immediately adjacent to the vein. Veins that host mineralization are composed largely of quartz and tourmaline, with accessory K-feldspar (perthite), plagioclase, cassiterite and wolframite, and trace apatite. Wolframite, cassiterite, tourmaline and, to a lesser extent, feldspar are intergrown in the veins. Cassiterite forms dark red, subhedral to anhedral crystals that are typically 1 cm and exceptionally 4 cm across, and wolframite occurs as coarse-grained euhedral blades up to 4 cm long. Tourmaline crystals in the veins attain a length of 4 cm, and are typically broken perpendicular to the *c* axis, with quartz \pm feldspar cementing the fragments. The quartz is unstrained

in some veins and highly deformed in others, as is the case in aplite and pegmatite. Muscovite is the most common secondary mineral in these veins, typically occurring as an incipient alteration of the feldspars, and with minor scheelite along fractures as a replacement of wolframite. Trace amounts of scheelite, and rare chalcopyrite, arsenopyrite, and pyrite, are observed along fractures in quartz and thus also postdate vein formation.

The feldspar mineralogy of the veins is comparatively simple. The plagioclase is typically untwinned albite with compositions ranging from An₀ to An₃ (Fig. 3), and Or contents of less than 1 mol%. The K-feldspar is perthitic, but contains fine-grained string exsolution of albite, rather than the coarse-grained lamellae that characterize much of the perthite in aplite and pegmatite. Intergrowths of vein-hosted cassiterite and K-feldspar or cassiterite and albite are defined by crystallographic faces, suggesting that the cassiterite and the feldspars were contemporaneously deposited from aqueous fluids.

An important feature of the veins is that they are discordant, contained within the aplite units, and terminate abruptly at the contacts between aplite and banded pegmatite (Fig. 6). As stated above, aplites and pegmatites are in sharp contact, and there is no evidence to suggest that differential shearing occurred along the contacts. The termination of veins at the aplite-pegmatite contacts therefore suggests that the aplite was at subsolidus conditions but that the pegmatite had not cooled sufficiently to sustain brittle fracture, *i.e.*, the

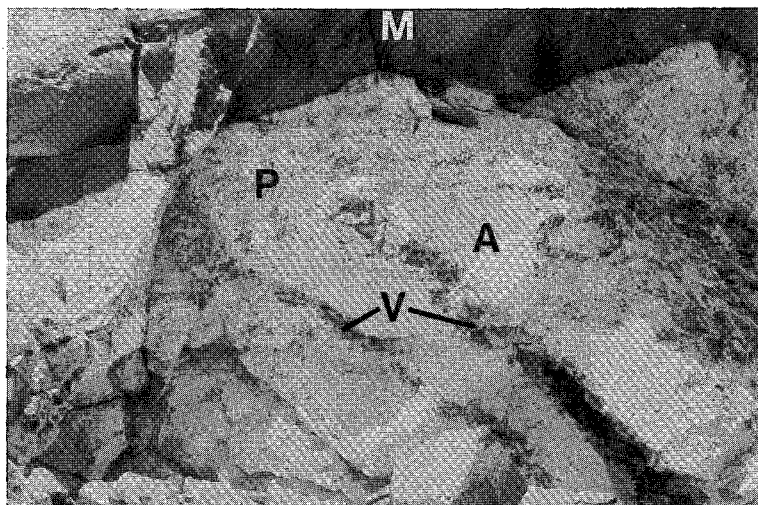


FIG. 6. Quartz-tourmaline veins cutting garnet aplite that terminate abruptly at the aplite-pegmatite contact. The abbreviations are: A aplite, M metasedimentary rocks, P pegmatite, V vein. The field of view is approximately 3 m across.

pegmatite was above or near solidus conditions during vein formation. A tourmaline layer in aplite, that continues through a quartz vein, is observed near section 9 (Fig. 2), in support of this interpretation. This feature is similar to the "phantom layering" through perthite crystals described by Jahns & Tuttle (1963). We interpret the phantom layering at Nong Sua similarly, and suggest that the aplite was locally at or above solidus conditions during vein formation, and that the tourmaline layer and quartz vein formed synchronously. In the same area, a late dyke of pegmatite cross-cuts a vein, indicating that there was at least some magmatic activity after vein formation. We therefore conclude that the veins formed from aqueous fluids liberated as the pegmatite-forming melt was achieving saturation in vapor, but before it had completely crystallized.

Greisen mineralization

A very small proportion of the mineralization occurs as cassiterite disseminated in pegmatite at the contacts with metasedimentary rocks and is classified as greisen. This cassiterite is in close spatial association with coarse-grained secondary muscovite and beryl. The muscovite has replaced the feldspars, and defines funnel-shaped zones that spread out along the contacts, but do not extend into the metasedimentary rocks. This is interpreted to reflect a hydrothermal process in which the metasedimentary rocks acted as an impermeable boundary and forced fluids to flow laterally.

Disseminated mineralization

Disseminated cassiterite in the banded pegmatite

unit, and less commonly in the garnet aplite unit, occurs in small patches (<0.5 m across) that have no discernible orientation. Mineralized pegmatites and aplites contain the highest grades of tin encountered in this study, but are otherwise similar to those barren of mineralization, *i.e.*, composed of quartz, K-feldspar, plagioclase \pm tourmaline \pm muscovite. The cassiterite is dark red, subhedral to euhedral, typically less than 1 cm across, and is intergrown with all pegmatite minerals and, in particular, tourmaline. Opaque inclusions are common in disseminated cassiterite but are extremely rare in vein-hosted cassiterite. The inclusions have been identified from results of electron-microprobe analyses as niobian-tantalum rutile, ilmenite, columbite and ixiolite. These minerals also are common to other pegmatite-hosted tin deposits in Thailand (Praditwan 1988). The opaque inclusions generally have irregular shapes; their abundance is highly variable amongst cassiterite crystals. These features suggest that the oxide inclusions in cassiterite did not originate by exsolution.

The contacts between disseminated cassiterite and plagioclase generally are sharp, defined by crystal faces. Locally, however, cassiterite seems to have been resorbed, and is embayed by plagioclase (Fig. 7a). The plagioclase in Figure 7a is oligoclase (An_{10}) and contains inclusions of cassiterite in the embayment. Cassiterite more commonly displays embayed contacts with perthite and myrmekite (Fig. 7b), and the feldspars at the embayed contacts also contain fine-grained inclusions of cassiterite. The myrmekite in Figure 7b is zoned (*cf.* Fig. 5), contains inclusions of cassiterite, and at the contact with the embayed crystal of cassiterite has a composition of An_{13} (the same as primary

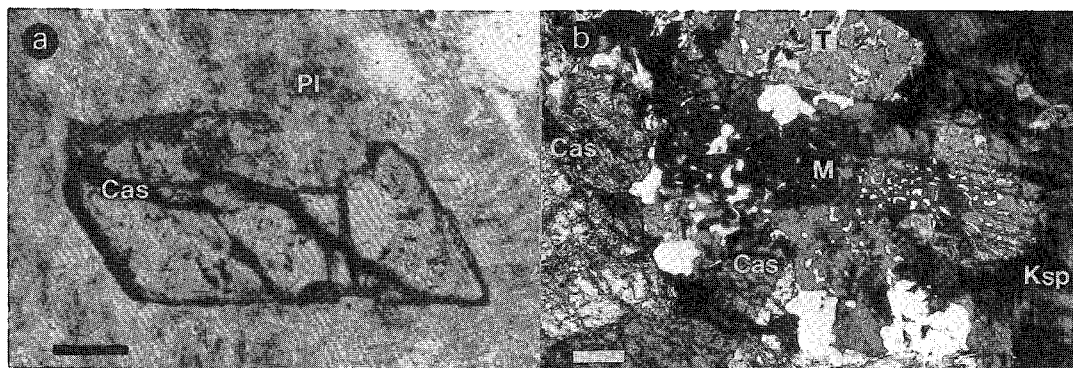


FIG. 7. Cassiterite-feldspar textures. a) Cassiterite (Cas) embayed by An_{10} plagioclase (Pl) (plane-polarized light). The bar scale represents 0.1 mm. b) Myrmekite (M) embayment of cassiterite (Cas) and perthite (Ksp); tourmaline (T) is also intergrown with cassiterite (cross-polarized light). The bar scale represents 0.25 mm.

plagioclase elsewhere in the same sample). These features suggest that cassiterite crystallization was penecontemporaneous with, but locally preceded, the crystallization of some of the primary plagioclase, and was followed by the formation of perthite and myrmekite.

STRUCTURAL AND COMPOSITIONAL DATA ON THE COEXISTING FELDSPARS

Ten representative specimens of aplite, pegmatite and vein were selected for further characterization of feldspar mineralogy. Various fractions were sampled individually for characterization by X-ray diffraction (powder method, Guinier-Hägg camera, synthetic spinel internal standard, $\text{CuK}\alpha_1$ radiation). Refinement of the unit-cell parameters in twenty-two subsamples was carried out using corrected and indexed diffraction-maxima, and the program of Appleman & Evans (1973), as modified by Garvey (1986). A listing of unit-cell dimensions of the coexisting feldspars in these ten samples is available from The Depository of Unpublished Data, CISTI, National Research Council, Ottawa, Ontario K1A 0S2. The unit-cell parameters have been used to obtain information of the composition and degree of Al-Si order of the feldspars (Table 1).

In all samples, the K-rich feldspar is microcline, as inferred from the presence of cross-hatched twinned domains. Whereas this finding is not unexpected for a body of granitic pegmatite, especially one subjected to deformation (Martin 1982), the degree of Al-Si order attained typically falls short of the perfect state of order that is expected. The value of t_1O is low (as low as 0.92) in the bulk of the megacrysts of grey and translucent perthite (t_1O is 1.00 in fully ordered microcline). Interestingly, the strongest peaks of orthoclase or of structurally intermediate microcline also are present in five of the seven subsamples of grey, translucent megacrystic perthite examined. Both intergrain heterogeneity in degree of Al-Si order attained in the microcline and the presence of more disordered phases point to a *relative* lack of low-temperature, fluid-mediated recrystallization in this suite. White, opaque portions of the microcline perthite grains, which are volumetrically minor, line cracks in and rim the deformed megacrysts; the white areas typically contain a more fully ordered microcline. The finer-grained assemblages (aplite, fine-grained tourmaline pegmatite) also contain the same range of N_{Or} and t_1O values for the microcline as the megacrysts. The suite contains microcline ranging in obliquity from 0.89 to 0.99 (Table 1).

The range of microcline compositions ($95 < N_{Or} < 99$; Table 1) reflects temperatures of final

TABLE 1. INDICATORS OF COMPOSITION AND DEGREE OF Al-Si ORDER IN K-RICH AND Na-RICH FELDSPARS IN REPRESENTATIVE SAMPLES OF THE NONG SUA APLITE-PEGMATITE COMPLEX

	K-rich feldspar				Na-rich feldspar		
	N_{Or}	t_1O	A	An	N_{Or}	t_1O	A131
PK-2a grey Kfs**	94.8	0.95	0.92	1	0.3	0.98	1.140
PK-2a feathery Kfs	97.3	0.99	0.95	2			1.143
PK-3b grey Kfs*	95.2	0.92	0.92	0	0.0	0.98	1.133
PK-3b white Kfs	96.6	1.00	0.97	2 ⁺			1.172
PK-3b matrix				13			1.367
PK-3b enclave				23			1.536
PK-3c grey Kfs	96.2	0.98	0.98	0 ⁺	0.4	0.98	1.146
PK-3c white Kfs	95.4	0.99	0.97	0	0.7	0.99	1.134
PK-3c aplite	98.3	0.98	0.81	3			1.174
PK-17a graphic granite	95.7	1.00	0.98	1	0.4	0.98	1.138
PK-17d grey Kfs	98.7	0.98	0.95	1	2.1	0.98	1.117
PK-17d white Kfs	95.0	0.99	0.98	0	0.0	0.98	1.113
PK-19a grey Kfs	95.9	0.98	0.97	0	0.0	0.98	1.059
PK-19a white Kfs	96.8	0.98	0.95	0	0.0	1.00	1.110
PK-33 grey-white Kfs	98.5	0.99	0.98	0	0.5	0.97	1.084
PK-33 cream Pl				10 ⁺			1.369
PK-46f white Kfs	96.5	1.00	0.99	0 ⁺	0.3	0.97	1.108
PK-46f Qtz-Tur vein				1	0.6	0.98	1.131
PK-54 Qtz-Tur vein	98.9	0.99	0.98	3 ⁺			1.019
PK-58 grey Kfs*	97.3	0.95	0.89	0 ⁺	0.9	0.90	1.103
PK-58 white rim	96.2	0.99	0.97	4			1.182
PK-58 aplite	94.9	0.98	0.93	11 ⁺			1.382

Composition N_{Or} is expressed in mole % Or, and was calculated using the equation of Kroll & Ribbe (1983) relating unit-cell volume to N_{Or} for feldspar compositions that are structurally ordered (i.e., that belong to the low microcline - low albite series). The degree of Al-Si order, expressed by t_1O , was computed using the equations of Blasi (1977). The error in N_{Or} and t_1O is believed to be ± 0.015 in most cases. The obliquity Δ of a microcline is equal to $12.5(\Delta_{131} - \Delta_{131}^0)$; it should have a value of 1.00 for fully ordered microcline. The $\Delta 131$ indicator of a plagioclase is the calculated angular separation of the 131 and 131 diffraction maxima, in 2θ ($\text{CuK}\alpha_1$ radiation). For a plagioclase more calcic than An_1 , as inferred by coordinates in the $\beta^* - \gamma^*$ diagram of Smith (1974, Fig. 7-44), values of N_{Or} and t_1O cannot be inferred using the indicators based on the low microcline - low albite series. * Evidence of residual disorder in plagioclase, based on coordinates in the $\beta^* - \gamma^*$ plot. ⁺ The strongest peaks of orthoclase also are present in the powder pattern. ⁺⁺ The strongest peaks of a structurally intermediate microcline also are present in the powder pattern. Grey and white subsamples were taken of perthite megacryst samples PK-3b, PK-3c, PK-17d, PK-19a and PK-58. Samples selected for study: PK-2a tourmaline aplite, PK-3b banded pegmatite-metasediment contact, PK-3c garnet aplite, PK-17a coarse-grained graphic quartz-K-feldspar, PK-17d coarse-grained K-feldspar (subhedral perthite), PK-19a coarse-grained graphic quartz-K-feldspar, PK-33 coarse-grained tourmaline-rich pegmatite, PK-46f quartz-tourmaline-feldspar-cassiterite-wolfraamite vein, PK-54 quartz-tourmaline-feldspar-wolfraamite vein, PK-58 garnet aplite.

equilibration between approximately 350° and 150°C or less. Values of N_{Or} closer to 95% are more prevalent in microcline from aplite and pegmatite (Table 1), which reinforces the inference made on structural grounds that this aplite-pegmatite system was not characterized by pervasive fluid-mediated recrystallization following deformation and accompanying cooling. The presence of perthite in the vein in which the low microcline is almost pure ($N_{Or} = 99$, Table 1) is consistent with continued hydrothermal re-equilibration of a high-temperature hydrothermally deposited orthoclase, at least in the case of vein PK-54.

The albite that coexists with microcline in the

grey, translucent perthite megacrysts (An_0 to An_2 and less than Or_1) presumably formed largely by exsolution at a temperature above the orthoclase-to-microcline transition, *i.e.*, above approximately 450°C. In some cases, albite, both as exsolution in perthite and as discrete crystals in veins, is characterized by residual Al-Si disorder (Table 1). It is also significant that much of the aplite- and pegmatite-hosted plagioclase is oligoclase (discussed above in light of electron-microprobe measurements; see also Table 1). In bodies of granitic pegmatite that have been subjected to an important internal circulation of aqueous fluid below about 400°C, such plagioclase would be expected to have been converted to a greenschist-facies assemblage of Ca-free albite + epidote. The persistence of oligoclase and of residual disorder in the albite is consistent with rapid cooling following emplacement, deformation and uplift, and general lack of low-temperature recrystallization.

INTERPRETATION OF FELDSPAR AND CASSITERITE TEXTURES

The fine grain-size of aplites has commonly been attributed to vapor loss (*e.g.*, Jahns & Tuttle 1963); in support of this interpretation, these textures have been experimentally reproduced in vapor-saturated granitic systems (*e.g.*, London *et al.* 1988). It thus seems likely that the aplites at Nong Sua crystallized largely under vapor-saturated conditions. There is much less consensus concerning the timing of vapor saturation in magmas that produce pegmatitic textures, although high contents of dissolved H_2O in these melts are generally considered to be fundamental. Of particular importance to the interpretation of the textures at Nong Sua are the experiments of Fenn (1986), London *et al.* (1989) and MacLellan & Trembath (1991), where graphic intergrowths of quartz and K-feldspar have been interpreted to reflect nonequilibrium growth (supersaturation) in melts that are vapor-undersaturated and water-bearing. Much of the coarse-grained K-feldspar at Nong Sua, including that graphically intergrown with quartz, formed after crystallization of oligoclase or calcic albite. If the graphic intergrowths at Nong Sua also formed at vapor-undersaturated conditions, most of the feldspar in the pegmatite units probably crystallized at vapor-undersaturated conditions. Additional support for this comes from the fact that myrmekite, including that graphically intergrown with quartz, formed after K-feldspar crystallization. This myrmekite cannot be metamorphic in origin, since evidence for a postmagmatic high-temperature metamorphic event is completely lacking in the surrounding metasedimentary rocks;

on the other hand, the replacement of K-feldspar by myrmekite indicates the involvement of a fluid phase but the preservation of intermediate structural states in the K-feldspar suggests that the fluid event must have been relatively short-lived. In addition, the compositional similarity of myrmekite to magmatic plagioclase at Nong Sua suggests that both crystallized at comparable conditions. We therefore conclude that myrmekite replacement of K-feldspar reflects the vapor saturation of the melt, which is supported by the "graphic-like" nature of the myrmekite. This interpretation is not unique, as myrmekite in similar environments is also interpreted as having originated during late vapor-saturation of a magma (Hibbard 1979, Hopson & Ramseier 1990).

The planarity of cassiterite-oligoclase contacts suggests penecontemporaneous growth, and the embayment of cassiterite by oligoclase (Fig. 7a) implies that some cassiterite crystallized before the end of plagioclase crystallization. The textural evidence therefore indicates that disseminated cassiterite crystallized directly from the melt. An alternative explanation is that the disseminated cassiterite precipitated from an aqueous fluid in a vapor-saturated melt (if vapor and melt are separated, the chemical potentials of tin in melt and fluid are not necessarily equal). The fact that disseminated cassiterite predates myrmekite (Fig. 7b) indicates that cassiterite probably began to crystallize at or near conditions of vapor saturation.

WHOLE-ROCK CHEMISTRY

If, as the textures suggest, the disseminated cassiterite indeed crystallized from the melt, evidence of such crystallization should be recorded by the petrochemistry of the aplite-pegmatite, in particular, by the distribution of tin. Four types of samples were therefore analyzed for major and trace elements: 1) garnet aplite, 2) fine-grained tourmaline-rich banded pegmatite, 3) coarse-grained K-feldspar-rich and graphic pegmatite, and 4) coarse-grained tourmaline-rich pegmatite. A single sample of plagioclase-rich aplite, from the banded pegmatite unit, also was analyzed. Average compositions for each of the sample types are listed in Table 2. Sample sizes ranged from 1 to 2 kg, and are probably representative of the aplite and fine-grained pegmatite. Compositions of the coarse-grained pegmatite units may not be representative; however, they represent, at worst, a mixture of lithologies and are still useful in assessing the behavior of tin during the evolution, and any subsequent alteration, of the pegmatitic rocks.

TABLE 2. AVERAGE WHOLE-ROCK COMPOSITIONS OF APLITE AND PEGMATITE

Type	Apl.	Ksp.	Tour.	Apl.BP.	BP.
n	9	7	4	1	4
SiO ₂ wt%	74.95	74.45	77.86	76.70	76.37
TiO ₂	0.04	0.02	0.08	0.02	0.06
Al ₂ O ₃	14.88	14.36	13.74	14.85	14.49
Fe ₂ O ₃	0.50	0.17	1.25	0.27	0.79
MnO	0.06	0.01	0.03	0.01	0.02
MgO	<0.01	<0.01	0.03	<0.01	<0.01
CaO	0.72	0.25	0.76	1.39	0.76
Na ₂ O	3.97	2.85	4.60	6.37	4.42
K ₂ O	4.28	7.60	1.16	0.42	2.87
P ₂ O ₅	0.05	0.05	0.03	0.05	0.04
LOI	0.59	0.25	0.50	0.29	0.45
Total	100.10	100.01	100.05	100.38	100.28
Ba ppm	13	15	15	38	16
Nb	27	10	52	35	39
Zr	23	3	16	28	13
Y	20	5	14	23	11
Sr	12	11	15	8	15
Rb	399	626	96	376	233
Pb	32	46	16	24	21
Th	8	5	8	8	11
F	384	107	483	140	385
Li	22	10	28	14	18
Ta	8	4	13	10	14
B	256	217	4133	389	1951
Sn	17	22	14	12	16
Norm					
q	34.09	28.34	45.06	35.20	38.14
or	25.27	44.94	6.87	2.48	16.96
ab	33.56	24.14	38.91	53.90	37.40
an	3.24	0.99	3.59	6.55	3.50
c	2.54	1.10	3.61	1.52	2.83
il	0.06	0.02	0.07	0.02	0.05
hem	0.43	0.17	1.25	0.27	0.79
ap	0.12	0.10	0.07	0.12	0.09
ru	0.01	0.01	0.04	0.01	0.04
hy	0.04	0.02	0.08	0.02	0.03
mt	0.11				

Apl. represents garnet aplite, Ksp. K-feldspar-rich pegmatite, Tour. tourmaline-rich pegmatite, Apl.BP. aplite contained within banded pegmatite, and BP. fine-grained tourmaline-rich banded pegmatite. Major elements and BaO were determined from fused pellets by X-ray fluorescence spectroscopy, with a detection limit of 0.01 wt%, and 10 ppm, respectively. Total iron is reported as Fe₂O₃. Most samples contain <0.01 wt% MgO; therefore median values are given. For TiO₂, MnO and P₂O₅, longer counting times were used to improve the detection limit to 0.001 wt%. Except for Sn, B, F, Ta and Li, the concentrations of trace elements were determined from pressed powder pellets by X-ray fluorescence, with detection limits of 3 ppm for Nb, Zr and Sr, and 5 ppm for the rest. Concentration of Sn was determined by NH₄I fusion and atomic absorption analysis, with a detection limit of 1 ppm. Three aplite samples contain visible cassiterite (53, 95, and 106 ppm Sn) and are excluded from the average. Concentration of B was determined by Na₂O₂ fusion and analysis by induced coupled plasma, with a detection limit of 2 ppm. Concentration of F was determined by NaOH fusion and analysis by specific ion electrode, with a detection limit of 10 ppm. Concentrations of Ta and Li were determined by induced coupled plasma analysis after 0.5 g of sample was digested with 10 mL of HClO₃-HNO₃-HF at 200°C and diluted with 10 mL of aqua regia. The detection limit of Ta and Li is 3 ppm. Also sought, but below detection limits, are V (<10 ppm), Ni (<10 ppm), Cr (<5 ppm), and U (<5 ppm).

Major- and trace-element relationships

The presence of primary muscovite, garnet and tourmaline indicates that the aplites and pegmatites

are peraluminous. This is also reflected by normative corundum, the values of which range from 0.79 to 5.08 wt.%. Figure 8 shows aplite and pegmatite compositions expressed in terms of normative quartz-orthoclase-albite and anorthite-orthoclase-albite. Most of the aplite and fine-grained tourmaline-rich pegmatite samples are similar in composition to the water-saturated minimum at 1 to 2 kbar in the haplogranite system. Other samples are either enriched or depleted in K-feldspar. In this respect, the compositions are comparable to those of other pegmatites (*cf.* Jahns & Tuttle 1963). Considering the coarse grain-size, the degree of scatter is relatively small. The absence of compositional shifts toward the Q or Ab corners on Figure 8 is consistent with the lack of petrographic evidence for significant greisenization or sodic metasomatism. It is difficult to assess potassic alteration using Figure 8, as pegmatite compositions trend toward the Or apex, but the lack of widespread replacement of plagioclase by K-feldspar suggests that potassic alteration was of limited importance in controlling whole-rock chemistry.

Most of the samples contain significant calcium and boron, both of which shift the composition of the granite minimum; the normative anorthite component is typically 3 to 4 wt.%, and B contents nearly attain 1 wt.% for tourmaline-rich pegmatite (average 4000 ppm, Table 2). The addition of anorthite as a component to the haplogranite system shifts minimum-melt compositions toward the quartz-orthoclase tie-line (James & Hamilton 1969), and excess aluminum, toward the quartz apex (Holtz *et al.* 1991), whereas the addition of boron shifts compositions toward the albite apex (Pichavant 1987). A comparison of the Nong Sua compositions with experimentally determined granite minimum-melt compositions therefore does not provide an estimate of pressure.

The dependence of proportions of major elements on the K-feldspar-to-plagioclase ratio is apparent if the major elements are plotted as oxides as a function of SiO₂. Figure 9 shows that K₂O and Al₂O₃ vary inversely, whereas Na₂O and CaO vary positively with increasing SiO₂. In terms of the alkali-to-aluminum ratio [expressed as molar (K + Na)/(K + Na + Al)], the most strongly peraluminous rocks are plagioclase-rich, almost devoid of K-feldspar. This is reflected, mineralogically, by the presence of primary muscovite and tourmaline in these rocks. Rocks having higher contents of K-feldspar have less strongly peraluminous compositions; the coarse-grained K-feldspar-rich units are metaluminous (Fig. 10a). The lack of widespread alteration is confirmed by the consistent variation in Rb/Sr with the alkali-to-aluminum ratio (Fig. 10b).

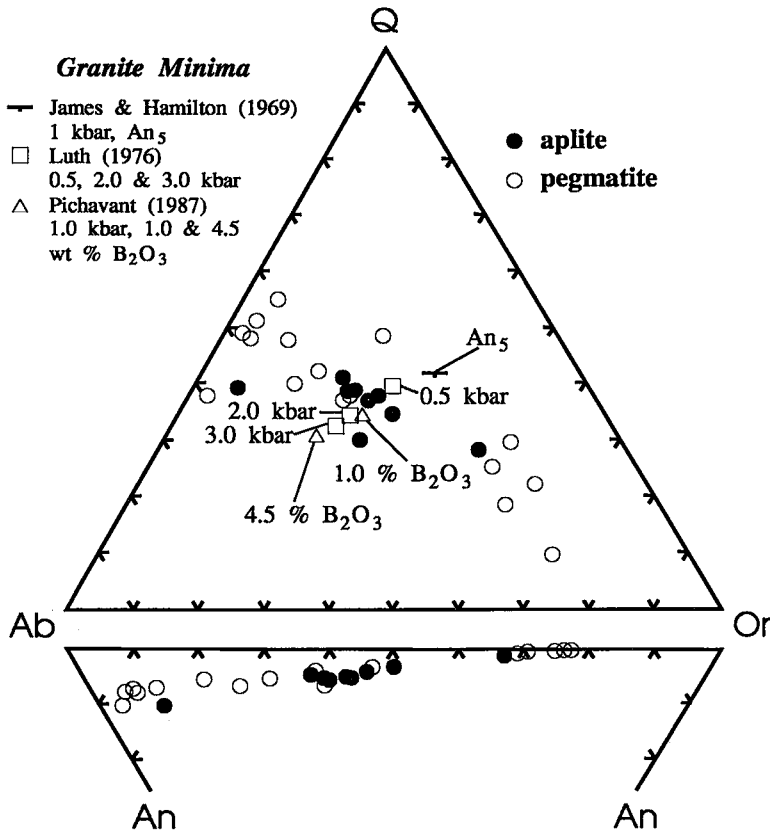


FIG. 8. Compositions of aplite and pegmatite expressed in terms of normative quartz (Q), albite (Ab), orthoclase (Or), and anorthite (An), and water-saturated granite minima for various pressures and compositions.

Boron concentration is inversely proportional to the alkali-to-aluminum ratio (Fig. 10c), which demonstrates the petrographic association of tourmaline with plagioclase-rich rocks. Figures 10d and 10e show similar trends for TiO₂ and Nb, which suggest that Ti and Nb were controlled largely by tourmaline abundance (oxide minerals are rare in non-mineralized aplite and pegmatite). In addition, strong positive correlations between B and Fe, Ta, F and Li concentrations indicate that these elements also were probably controlled dominantly by tourmaline (tourmaline pegmatite also contains primary muscovite). However, the Ta/(Ta + Nb) ratio displays the opposite trend, increasing with increasing alkali-to-aluminum value (Fig. 10f). This ratio, used as a measure of fractionation (Černý *et al.* 1985, Jolliff *et al.* 1992), suggests that the tourmaline-rich units may be less evolved.

Distribution of tin

It is possible to evaluate the behavior of tin during granite evolution and the effects of subsolidus alteration on its remobilization by plotting the concentration of Sn *versus* parameters such as TiO₂ and Rb/Sr, which can in turn be related to the degree of fractionation (Lehmann 1990). Although cassiterite-feldspar textures suggest that the pegmatite-forming melt was saturated in cassiterite, the tin contents of cassiterite-bearing samples are difficult to interpret owing to the inhomogeneous distribution of cassiterite and the related problem of sample size. The relationships between tin abundances and compositions in terms of major elements, discussed below, are therefore based only on samples that are free of cassiterite; data on three samples of aplite that contain trace

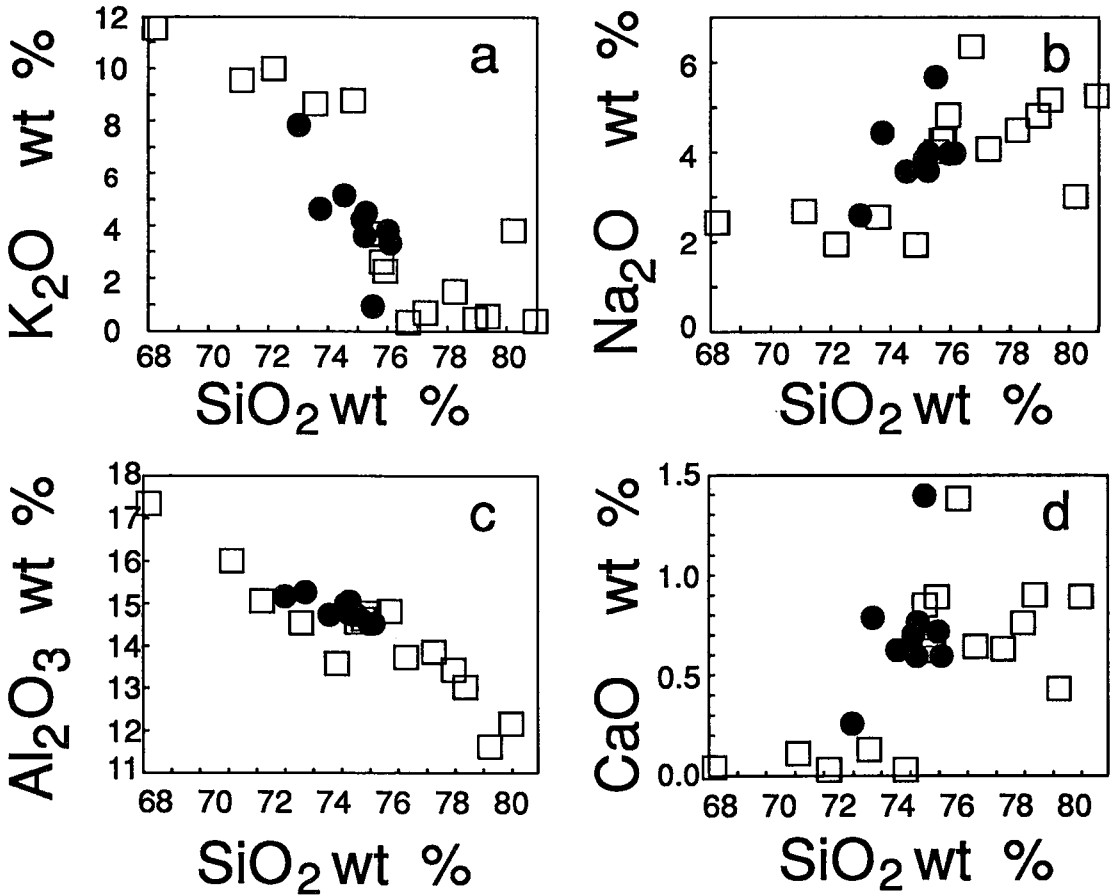


FIG. 9. Compositions of aplite (solid circles) and pegmatite (open squares) expressed in terms of weight percent K₂O, Na₂O, Al₂O₃, and CaO versus SiO₂.

disseminated cassiterite are excluded (in terms of major- and trace-element chemistry, these samples are otherwise similar to cassiterite-free aplite).

Most granitic suites contain progressively less Sr and Ba and more Rb as a result of fractionation. At Nong Sua, Rb contents vary from 37 to 995 ppm, Sr from 7 to 18 ppm, and Ba from <10 to 48 ppm. The melt-feldspar partition coefficients for Rb are in favor of K-feldspar over plagioclase (Smith 1974), which is reflected by the strong correlation between Rb and K₂O (Fig. 11a). This correlation, and that between log Sr and log Rb/Sr, further suggest that the Rb-Sr distribution has not been affected by alteration. The wide range of log Rb/Sr and restricted range of log Sr values (Fig. 11b) undoubtedly reflect differences in the plagioclase to K-feldspar ratios among the samples analyzed. This is not unusual, since a near-constant and low abundance of Sr with variable Rb

concentrations is interpreted elsewhere as being indicative of highly fractionated melts (Walker *et al.* 1986), and similar Rb-Sr relationships are reported for pegmatites elsewhere (*e.g.*, Černý *et al.* 1984, Trumbull 1991).

The behavior of Sn in granitic suites is dependent on the $f(\text{O}_2)$ of the melt. In oxidized melts, tin, in the 4+ valence, substitutes in minerals such as magnetite and is not concentrated by fractionation. By contrast, in reduced granites, tin is dominantly divalent, and its abundance increases with fractionation (*cf.* Lehmann 1990). The values of the log Sn concentration of the Nong Sua samples correlate positively with those of log Rb/Sr and negatively with those of log TiO₂, similar to the fractionation trends proposed by Lehmann & Mahawat (1989) for western Thai granites, but at lower abundances of Sn (Figs. 11c, d). The small degree of scatter suggests that significant

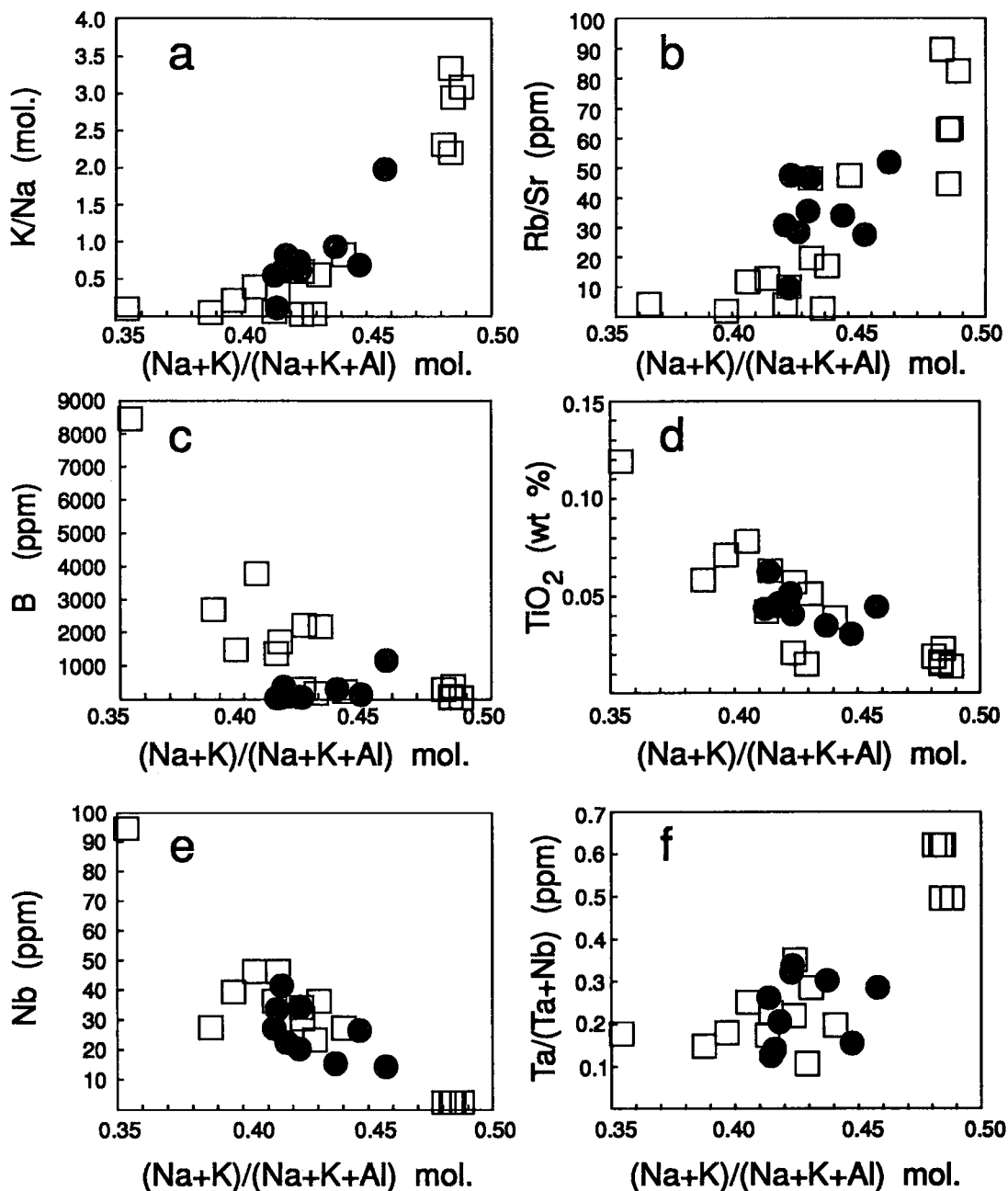


FIG. 10. Alkali-to-aluminum values $[(Na+K)/(Na+K+Al)]$ of aplite (solid circles) and pegmatite (open squares) expressed in terms of a) K/Na, b) Rb/Sr, c) B, d) TiO₂, e) Nb, and f) Ta/(Ta+Nb).

hydrothermal remobilization of tin did not occur, and that the assumption that these rocks are cassiterite-free is probably valid. Since tin behaves

as an incompatible element in suites of unaltered S-type granite, it is also likely that tin behaves as an incompatible element during the internal

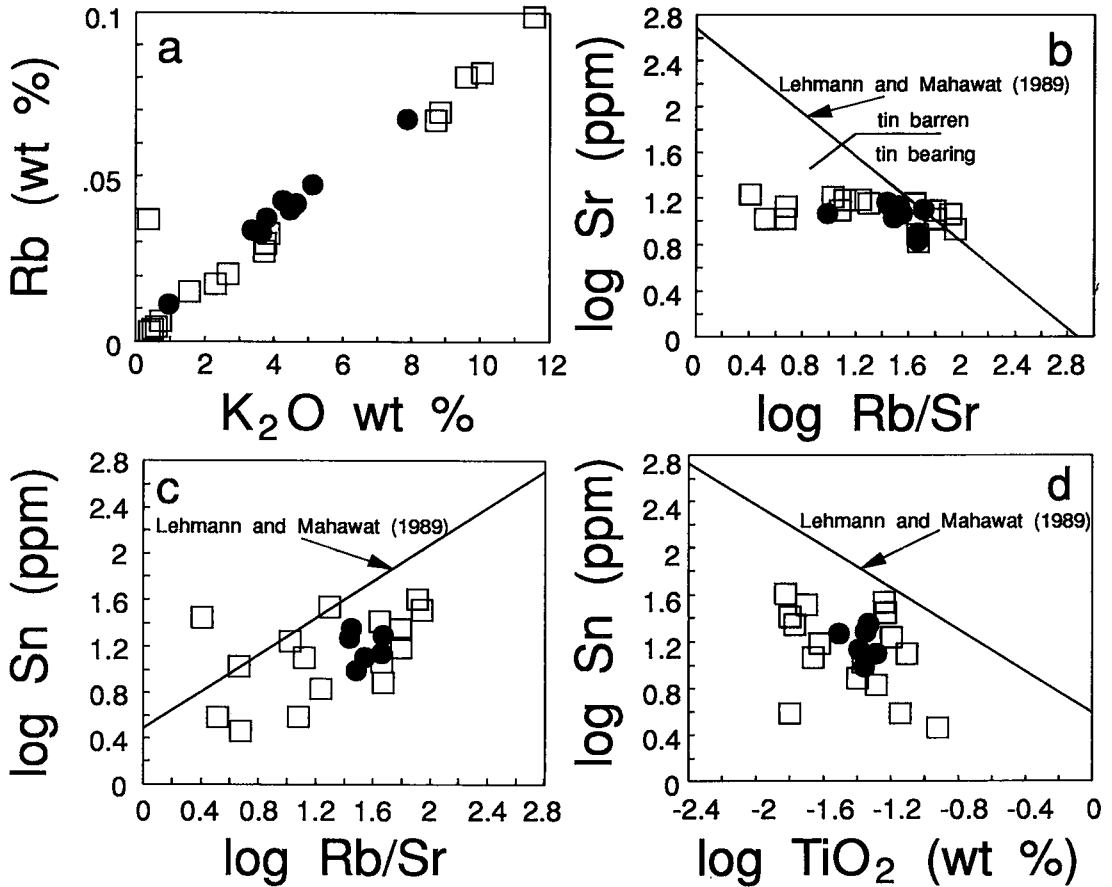


FIG. 11. Compositions of nonmineralized aplite (solid circles) and pegmatite (open squares). The reference lines of Lehmann & Mahawat (1989) are regressed from compositions of granites in western Thailand; the tin-barren *versus* tin-bearing fields are also from that study. a) Rb *versus* K₂O. b) Log Sr *versus* log Rb/Sr. The reference line indicates the change of granite composition, with log Rb/Sr increasing with fractionation. Nong Sua compositions reflect highly fractionated melts and do not follow this trend. c) Log Sn *versus* log Rb/Sr and d) log Sn *versus* log TiO₂. Nong Sua compositions in c and d delineate trends similar to the granite trends of Lehmann & Mahawat (1989). In the latter study, increasing abundance of tin was interpreted to reflect increasing fractionation.

development of peraluminous pegmatites, *i.e.*, the most evolved rocks at Nong Sua contain the highest concentrations of tin.

Figure 12 shows the distribution of Sn *versus* concentrations of the major elements, expressed as oxides. Tin is positively correlated with Al₂O₃ and K₂O, and is negatively correlated with SiO₂. Similar diagrams were constructed for B and F; these elements do not correlate with concentrations of tin and thus did not affect its distribution. In terms of the alkali-to-aluminum ratio, the most peraluminous rocks have the lowest concentrations of Sn, and the metaluminous rocks (K-rich) have

the highest abundances. The metaluminous K-rich samples are mainly composed of K-feldspar and quartz, and lack tourmaline and muscovite. Despite the fact that the concentration of tourmaline and muscovite might be expected to control whole-rock abundance of tin (see below), the distribution of tin in nonmineralized aplite-pegmatite is apparently related to K-feldspar abundance.

APLITE-PEGMATITE EVOLUTION AND CASSITERITE CRYSTALLIZATION

A growing body of natural and experimental

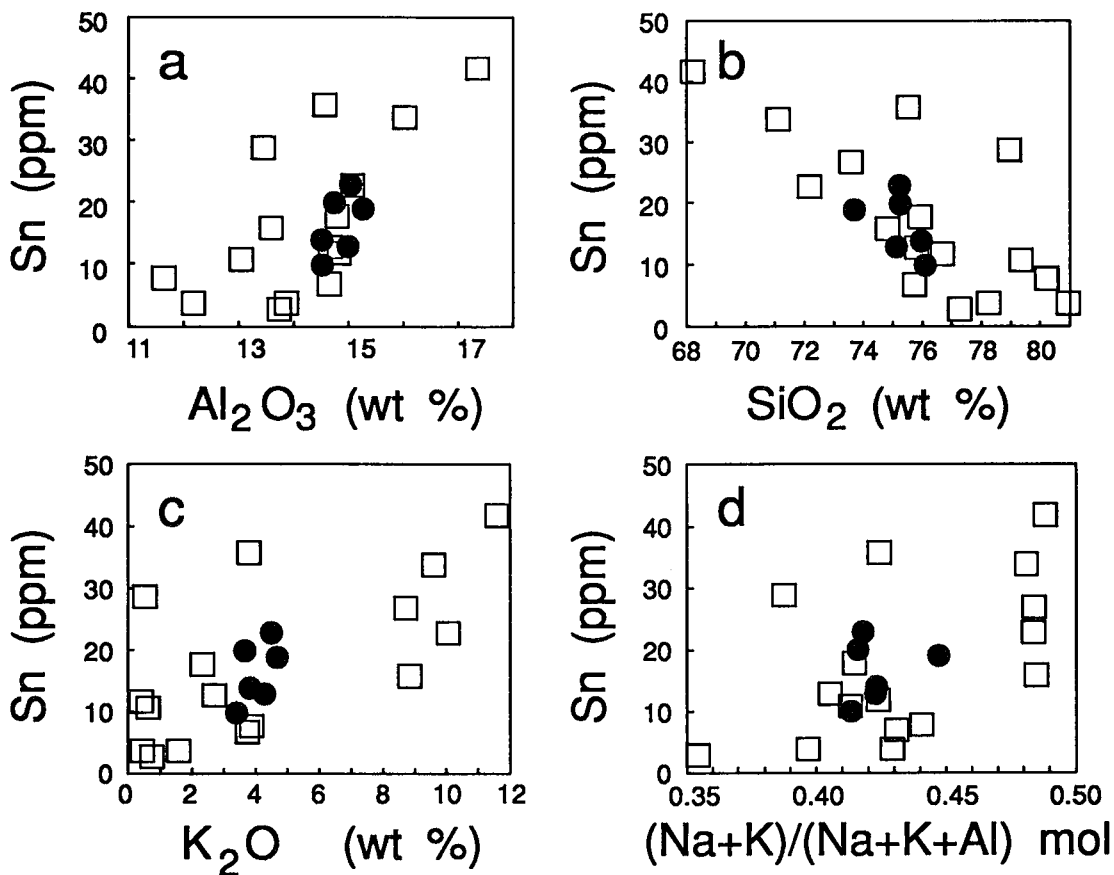


FIG. 12. Distribution of tin in nonmineralized aplite (solid circles) and pegmatite (open squares) in terms of a) Al_2O_3 , b) SiO_2 , c) K_2O , and d) the molar $(\text{Na}+\text{K})/(\text{Na}+\text{K}+\text{Al})$ ratio.

data suggests that the origin of layering in granites and pegmatites is a consequence of supersaturation and rapid growth of crystals (*e.g.*, Rockhold *et al.* 1987, London *et al.* 1989). These models offer an alternative to the Jahns & Burnham (1969) model, which invokes vapor transport, in particular that of potassium, to explain pegmatite layering. In all of these models, the pegmatite units can be considered to represent cumulates; this makes partition-coefficient data, especially for trace elements, extremely important. Although partition data are sparse, they are nevertheless sufficient to permit rough interpretation of the whole-rock data. The aplites at Nong Sua consistently have compositions that are intermediate between those of K-rich and K-poor pegmatites. The close chemical relationship of aplite and pegmatite supports the conclusion, based on field relations, that aplite and pegmatite both crystallized from a single batch of

magma. In general, if a granitic melt has evolved to a minimum-melt composition, further crystallization will have little effect on the major-element composition. However, trace-element composition can vary significantly with continued crystallization, particularly if the melt structure (and hence partition coefficients) change with evolution. The major-element compositions of the Nong Sua aplites can therefore be considered to represent minimum-melt compositions (*i.e.*, liquids), whereas the abundances of trace elements may also reflect the effects of mineral accumulation (*i.e.*, the melt's composition can only be calculated from partition coefficients).

The timing of crystallization of the different pegmatite units at Nong Sua is poorly constrained, except that K-feldspar is commonly late. Since graphic quartz - K-feldspar and discrete grains of K-feldspar within units were late in the paragenetic

sequence, the graphic and coarse-grained K-feldspar units probably also were late, although the banded nature of the pegmatite suggests that the sequence of crystallization may have been repeated. It thus follows that the most alkaline (metaluminous, K-rich) units at Nong Sua were the last to crystallize. This evolution is similar to the "liquid line of descent" proposed by London *et al.* (1989), wherein pegmatite evolution was modeled by decreasing SiO_2 and increasing alkali elements. Such an evolution for the Nong Sua pegmatite not only explains the textural relationships, but also the lower TiO_2 and the higher Sn and Ta/(Ta+Nb) ratios observed in the K-rich units.

Solubility of tin

The above discussion suggests that tin behaved as an incompatible element in the pegmatite-forming melts at Nong Sua. The systematic variation of tin in aplite and pegmatite also indicates that significant tin was not remobilized as a result of alteration of silicates or oxides. Although magmatic processes clearly controlled the distribution of tin in the nonmineralized aplite and pegmatite, it remains to be shown whether or not the tin abundances at Nong Sua are consistent with cassiterite saturation, in light of the available data on the solubility of tin in granitic magmas. It should be noted that, since the samples examined are nonmineralized, the highest estimates of tin contents in melt should reflect a slight undersaturation of cassiterite. In a summary of experimental work, Štemprok (1990) concluded that the dominant control of Sn solubility in granitic melts is temperature. In contrast, Naski & Hess (1985) and Taylor & Wall (1992) concluded that the dominant controls of tin solubility in granitic melts are the (Na+K)/Al and K/Na ratios and $f(\text{O}_2)$. The latter authors also suggested that Sn may occur as an alkali complex, of the type that has been proposed for other high-field-strength elements such as Ti (Dickinson & Hess 1985). Although the effect of melt structure on mineral-melt partition coefficients for tin is not known, the strong correlation between K and Sn at Nong Sua indicates that such complexing may be important at supersolidus conditions.

According to the solubility data of Štemprok (1990), approximately 850 and 1900 ppm Sn are required to saturate a melt in cassiterite at 600° and 700°C, respectively. The experimental data of Taylor & Wall (1992) predict somewhat different solubilities of cassiterite. At 700° to 800°C, 2 to 3 kbar, and $f(\text{O}_2)$ at FMQ to FMQ + 1.5 log units, cassiterite saturation occurs between 400 and 2500 ppm Sn. Tin solubility in these experiments was found to increase with increasing (Na+K)/Al and

Na/K ratios and with decreasing $f(\text{O}_2)$. All the values of cassiterite saturation reported above are much higher than the Sn contents of aplites and pegmatites at Nong Sua (Table 2). However, since tin was concentrated by fractionation, the bulk distribution coefficient was less than 1, and the concentration of tin in the rock is less than that in the melt from which it crystallized.

Partitioning of tin

Experimental studies of mineral-melt partition coefficients for tin are unfortunately lacking. However, Kovalenko *et al.* (1988) proposed partition coefficients based on empirical data. For the minerals observed at Nong Sua, the partition coefficients are $K_{\text{mica}}^{\text{Sn}} > 1 > K_{\text{plagioclase}}^{\text{Sn}} > K_{\text{K-feldspar}}^{\text{Sn}} > K_{\text{quartz}}^{\text{Sn}}$. Using these partition coefficients and whole-rock compositions, it is possible to estimate the concentration of tin in the melt at Nong Sua. The pegmatites with the highest tin contents are composed of $\geq 98\%$ perthite + quartz (Fig. 12) and contain, on average, 28 wt.% normative quartz. The average tin content of these pegmatites is 22 ppm (Table 2), and that of individual samples attains 42 ppm. The tin content of the melt was calculated using normative quartz and perthite (Or + An + Ab) and their respective partition coefficients at 600° and 700°C (Kovalenko *et al.* 1988); we assumed that all the tin is contained in quartz and K-feldspar (as indicated by the K_2O -Sn correlation). Concentrations of Sn estimated to have been in the melt are 391 and 253 ppm at 600° and 700°C, respectively, for the average K-feldspar-rich pegmatite. These concentrations are below the cassiterite saturation values of Taylor & Wall (1992) and Štemprok (1990), which suggests that during much of the pegmatite's evolution, cassiterite had not achieved saturation. The sample with the highest content of tin (42 ppm; 13% normative quartz) is estimated to have been in equilibrium with a melt containing 667 ppm Sn at 600°C and 444 ppm at 700°C. These values are in the range of saturation values quoted by Taylor & Wall (1992) and are close to those of Štemprok (1990). Since these values were obtained from nonmineralized samples, we conclude that further crystallization, or change of intensive parameters, particularly an increase in $f(\text{O}_2)$, resulted in crystallization of cassiterite from the melt.

It is important to note that the lowest abundances of tin occur in the most strongly peraluminous rocks, those containing tourmaline and muscovite. In light of the relative order of the above mineral-melt partition coefficients, the peraluminous rocks must have crystallized from a melt with much lower Sn concentrations, in accord with the interpretation that the peraluminous units

formed early and were followed by metaluminous units. The degree of fractionation required to account for a concentration of 700 ppm Sn in the melt can be estimated using the Rayleigh fractionation equation:

$$C_1 = F^{(D-1)} \times C_0^i$$

where C_1 is the concentration of tin in the fractionated melt, C_0^i is the concentration of tin in the initial melt, D is the bulk solid-melt distribution coefficient, and F is the proportion of melt remaining. Bulk distribution coefficients of 0.1 to 0.3 probably are reasonable (*cf.* Coetzee & Twist 1989); since the aplites of Nong Sua have an average tin content of 17 ppm (Table 2), the initial melt is estimated to have had 50 ($D = 0.1$) to 100 ($D = 0.3$) ppm Sn. At a C_0^i of 50 ppm Sn, 95 to 98% fractionation is required to attain 700 ppm Sn in the melt, or at a C_0^i of 100 ppm Sn, 88 to 94% fractionation is required ($0.1 < D < 0.3$). It therefore follows that the crystallization of cassiterite at Nong Sua probably occurred after more than 90% of the crystallization of the aplite-pegmatite was completed.

Effect of vapor saturation

The above calculations do not consider the effects of vapor saturation, which potentially changed the bulk distribution coefficient. The occurrence of vein-hosted and greisen styles of mineralization are evidence that the hydrothermal fluids contained significant concentrations of tin. The lack of alteration of aplite and pegmatite indicates that these fluids did not leach tin from the wallrock, which implies that tin was partitioned into the orthomagmatic fluid upon vapor saturation. However, even if $K_{\text{fluid-melt}}^{\text{Sn}}$ was less than 1.0, hundreds of ppm Sn could still have been in solution, given that the melt contained on the order of 700 ppm Sn. Taylor (1988) found that the partition coefficient for tin between vapor and haplogranitic melt ($K_{\text{fluid-melt}}^{\text{Sn}}$), derived from experimental studies, is proportional to the square of the aqueous chloride molality and that $K_{\text{fluid-melt}}^{\text{Sn}}$ is greater than 1.0 if the chloride concentration is greater than approximately 1 molar. Durasova *et al.* (1986) also found that $K_{\text{fluid-melt}}^{\text{Sn}}$ is proportional to chloride concentration, but estimated that the $K_{\text{fluid-melt}}^{\text{Sn}}$ for a 1 N Cl solution coexisting with haplogranite is 0.2, at 750°C and 1.5 kbar, at the Ni-NiO buffer. Keppler & Yllie (1991) estimated a $K_{\text{fluid-melt}}^{\text{Sn}}$ of less than 0.1 for haplogranite at 750°C, 2 kbars, at the Ni-NiO buffer. Discrepancies among the experimental results may, in part, have resulted from high solubilities of tin in the noble metals used as capsules. However, there is sufficient agreement to conclude that, for chlorinities of less than 1 M, $K_{\text{fluid-melt}}^{\text{Sn}}$ is less than

1.0 in granitic systems. At Nong Sua, the orthomagmatic fluid is considered to have had a low salinity (< 1 M; Linnen & Williams-Jones 1991). Tin, therefore, was not strongly partitioned into this fluid. Since the mass of fluid at vapor saturation was small compared to the mass of melt, and $K_{\text{fluid-melt}}^{\text{Sn}}$ was less than 1.0, vapor saturation would have had only a minor effect on the bulk distribution coefficient and thus on the tin content of the melt (calculated above). In addition, the fact that $K_{\text{fluid-melt}}^{\text{Sn}}$ was less than 1.0 implies that some cassiterite must have crystallized directly from the late-stage granitic melt at Nong Sua, regardless of the timing of vapor saturation.

LATE-STAGE EVOLUTION OF PEGMATITE

It was demonstrated above that samples of nonmineralized K-rich pegmatite are close to being saturated with cassiterite. This, however, does not explain why disseminated cassiterite is associated with pegmatite containing both K-feldspar and plagioclase, why disseminated cassiterite is typically associated with tourmaline, and why Ti-Nb-Ta oxide minerals are abundant as inclusions in disseminated cassiterite but are absent in vein cassiterite. The saturation of the granitic melt in vapor potentially explains these characteristics. Lowering the water content of the melt by vapor saturation raises the solidus temperature and promotes crystallization. If boron is partitioned into the vapor phase, the solubility of water in the remaining melt is further reduced (Pichavant 1987); thus water saturation of a boron-rich melt is an effective mechanism of quenching. Although the boron content of Nong Sua melts could not have been extraordinarily high, if buffered by the crystallization of tourmaline, vapor saturation nevertheless could have been an effective mechanism of quenching. The K-rich units are interpreted as cumulates, resulting from crystal growth at supersaturated conditions. The melt from which this unit crystallized also contained Na and B, for example, that are not reflected by the cumulate composition since plagioclase and tourmaline were not crystallizing. But, upon quenching, a composition closer to the granite minimum should have resulted (*i.e.*, a composition closer to that of the liquid, than that of the K-rich cumulate) as is the case for the host to the disseminated mineralization. The release of boron into aqueous fluids is evident by the formation of quartz-tourmaline veins and by the presence of tourmaline as an alteration mineral in metasedimentary rocks at the pegmatite contacts. Tourmaline intergrown with disseminated cassiterite may have had either a magmatic or hydrothermal origin; fluctuations between saturation and undersaturation of cas-

ssiterite at vapor-saturated melt conditions may explain the etching (embayment) of cassiterite, which was later filled by plagioclase or perthite (the feldspars also potentially crystallized either from silicate melt or aqueous fluids). Furthermore, Ti, Ta and Nb in the residual melt must have either been forced to crystallize as minerals or partition into the aqueous phase. The lack of Ti-Ta-Nb oxide minerals in vein cassiterite (or as accessory minerals in the quartz-tourmaline veins) indicates that these elements were not highly mobile. The inclusions of niobian-tantalian rutile, ixiolite and columbite in disseminated cassiterite are therefore interpreted to reflect the quenching process.

We propose that the quenching also resulted in fluid overpressure in the latest magma. This caused brittle failure in the aplite, and the formation of quartz-tourmaline \pm cassiterite \pm wolframite veins. The pegmatite was, at least locally, super-solidus and thus did not deform by brittle failure. However, the features of brittle and ductile deformation, developed locally in aplite, pegmatite and veins, also are interpreted to have formed at this stage, or during the early subsolidus evolution (indicated by stress-related perthite exsolution above approximately 450°C, the temperature of the orthoclase-to-microcline transition). A fluid-assisted tectonic overprint of the aplite-pegmatite complex can be ruled out on the basis of the preservation of intermediate structural states in K-feldspar (K-feldspar would have equilibrated to maximum microcline during a tectonic overprint) and of oligoclase.

Given that the veins and pegmatite crystallized at similar P-T conditions, it remains to be explained why the vein plagioclase is albite (An₀ to An₃), whereas oligoclase is observed in pegmatite. The composition of plagioclase crystallizing from the aqueous fluids was dependent on T, P and, in particular, fluid composition. In general, the Ca/Na ratio of fluid coexisting with melt is strongly dependent on chlorinity, and for the low-salinity fluids at Nong Sua (*cf.* Linnen & Williams-Jones 1991), the Ca/Na ratio of the fluid would have been much lower than that of the melt (*cf.* Candela 1989). Similarly, plagioclase that crystallized from the orthomagmatic fluid would have had a very low Ca/Na ratio (Schliestedt & Johannes 1990). Therefore, the albite observed in veins that host cassiterite at Nong Sua could have formed from hydrothermal fluid while the final granitic magma was above or near solidus conditions.

CONCLUSIONS

The crystallization of the Nong Sua complex commenced with the formation of aplite with a granitic composition. Pegmatite crystallized later to

form units with strongly contrasting compositions. The K-feldspar-rich units are interpreted to be late, relative to the plagioclase-tourmaline-rich units. Tin abundance increases with potassium content, suggesting that the tin concentration of the melt increased with fractionation. The textural relationships between cassiterite, plagioclase and myrmekite imply that cassiterite crystallized prior to or at vapor-saturated melt conditions. This interpretation has been tested by comparing the calculated abundance of tin in the melt with experimentally determined limits of tin solubility; we conclude that the melt contained on the order of 700 ppm Sn, which is consistent with the crystallization of primary cassiterite. Mineralization continued after vapor saturation to form vein-hosted cassiterite and wolframite, and greisen cassiterite. In the case of the former, the timing of mineralization is constrained, by cross-cutting relationships, to have been at or near solidus conditions of the pegmatite. The hydrothermal stage at Nong Sua was relatively short-lived, as indicated by the preservation of intermediate structural states in K-feldspar and the presence of oligoclase. However, as a consequence of fluid overpressure, brittle failure occurred in the aplite units, resulting in the formation of veins, and features of brittle and ductile deformation were developed locally in aplite, pegmatite and veins.

ACKNOWLEDGEMENTS

This research was carried out with the aid of a grant from the International Development Research Centre, Ottawa. We thank S. Bunopas, N. Jungyusuk, S. Khositanont, and P. Putthapiban of the Geological Survey Division, Department of Mineral Resources of Thailand for their support during the course of this project. The manuscript was improved by comments from D. Baker, J. Clark, B. Lehmann, R.P. Taylor and an anonymous referee, and from discussions with F. Holtz and M. Pichavant.

REFERENCES

- APPLEMAN, D.E. & EVANS, H.T., JR. (1973): Job 9214: indexing and least-squares refinement of powder diffraction data. *U.S. Geol. Surv., Comput. Contrib.* **20** (NTIS Doc. PB2-16188).
- BLASI, A. (1977): Calculation of T-site occupancies in alkali feldspar from refined lattice constants. *Mineral. Mag.* **41**, 525-526.
- CANDELA, P.A. (1989): Magmatic ore-forming fluids: thermodynamic and mass transfer calculations of metal concentrations. *In* Ore Deposits Associated with Magmas (J.A. Whitney & A.J. Naldrett, eds.). *Rev. Econ. Geol.* **4**, 203-221.

- ČERNÝ, P., MEINTZER, R.E. & ANDERSON, A.J. (1985): Extreme fractionation in rare-element granitic pegmatites: selected examples of data and mechanisms. *Can. Mineral.* **23**, 381-421.
- _____, SMITH, J.V., MASON, R.A. & DELANEY, J.S. (1984): Geochemistry and petrology of feldspar crystallization in the Vezna pegmatite, Czechoslovakia. *Can. Mineral.* **22**, 631-651.
- CHARUSIRI, P. (1989): *Lithophile Metallogenetic Epochs of Thailand: a Geological and Geochronological Investigation*. Ph.D. thesis, Queen's Univ., Kingston, Ontario.
- COBBING, E.J., MALLICK, D.I.J., PITFIELD, P.E.J. & TEOH, L.H. (1986): The granites of the southeast Asian tin belt. *J. Geol. Soc. London* **143**, 537-550.
- COETZEE, J. & TWIST, D. (1989): Disseminated tin mineralization in the roof of the Bushveld granite pluton at the Zaaiploats mine, with implications for the genesis of magmatic hydrothermal tin systems. *Econ. Geol.* **84**, 1817-1834.
- DICKINSON, J.E. & HESS, P.C. (1985): Rutile solubility and titanium coordination in silicate melts. *Geochim. Cosmochim. Acta* **49**, 2289-2296.
- DURASOVA, N.A., RYABCHIKOV, I.D. & BARSUKOV, V.L. (1986): The redox potential and the behavior of tin in magmatic systems. *Int. Geol. Rev.* **28**, 305-311.
- FENN, P.M. (1986): On the origin of graphic granite. *Am. Mineral.* **71**, 325-330.
- GARVEY, R. (1986): LSUCRIPC, least squares unit-cell refinement with indexing on the personal computer. *Powd. Diff.* **1**(1), 114.
- HIBBARD, M.J. (1979): Myrmekite as a marker between preaqueous and postaqueous phase saturation in granitic systems. *Geol. Soc. Am. Bull.* **90**, 1047-1062.
- HOLTZ, F., JOHANNES, W. & PICHAVANT, M. (1991): Effect of excess aluminium on phase relations in the system Qz-Ab-Or: experimental investigation at 2 kbar and reduced H₂O-activity. *Eur. J. Mineral.* **4**, 137-152.
- HOPSON, R.F. & RAMSEYER, K. (1990): Cathodoluminescence microscopy of myrmekite. *Geology* **18**, 336-339.
- JAHNS, R.H. & BURNHAM, C.W. (1969): Experimental studies of pegmatite genesis. I. A model for the derivation and crystallization of granitic pegmatites. *Econ. Geol.* **64**, 843-864.
- _____, & TUTTLE, O.F. (1963): Layered pegmatite-aplite intrusives. *Mineral. Soc. Am., Spec. Pap.* **1**, 78-92.
- JAMES, R.S. & HAMILTON, D.L. (1969): Phase relations in the system NaAlSi₃O₈-KAlSi₃O₈-CaAl₂Si₂O₈-SiO₂ at 1 kilobar water vapour pressure. *Contrib. Mineral. Petrol.* **21**, 111-141.
- JOLLIFF, B.L., PAPIKE, J.J. & SHEARER, C.K. (1992): Petrogenetic relationships between pegmatite and granite based on geochemistry of muscovite in pegmatite wall zones, Black Hills, South Dakota, USA. *Geochim. Cosmochim. Acta* **56**, 1915-1939.
- KEPLER, H. & WYLLIE, P.J. (1991): Partitioning of Cu, Sn, Mo, W, U, and Th between melt and aqueous fluid in the systems haplogranite-H₂O-HCl and haplogranite-H₂O-HF. *Contrib. Mineral. Petrol.* **109**, 139-150.
- KOVALENKO, V.I., RYABCHIKOV, I.D. & ANTIPIN, V.S. (1988): Temperature dependence of the distribution coefficients for Sn, W, Pb, and Zn, in magmatic systems. *Geochem. Int.* **25**, 1-10.
- KROLL, H. & RIBBE, P.H. (1983): Lattice parameters, composition and Al,Si order in alkali feldspars. In *Feldspar Mineralogy* (second edition, P.H. Ribbe, ed.). *Rev. Mineral.* **2**, 57-99.
- LEHMANN, B. (1990): *Metallogeny of tin*. Springer-Verlag, New York.
- _____, & MAHAWAT, C. (1989): Metallogeny of tin in central Thailand: a genetic concept. *Geology* **17**, 426-429.
- LINNEN, R.L. & WILLIAMS-JONES, A.E. (1991): Magmatic cassiterite mineralization at Nong Sua, Thailand. In *Source, Transport and Deposition of Metals* (M. Pagel & J.L. Leroy, eds.). Balkema, Rotterdam, The Netherlands (767-770).
- LONDON, D., HERVIG, R.L. & MORGAN, G.B., VI (1988): Melt-vapor solubilities and elemental partitioning in peraluminous granite-pegmatite systems: experimental results with Macusani glass at 200 MPa. *Contrib. Mineral. Petrol.* **99**, 360-373.
- _____, MORGAN, G.B., VI & HERVIG, R.L. (1989): Vapor-undersaturated experiments with Macusani glass + H₂O at 200 MPa, and the internal differentiation of granitic pegmatites. *Contrib. Mineral. Petrol.* **102**, 1-17.
- LUTH, W.C. (1976): Granitic rocks. In *The Evolution of Crystalline Rocks* (D.K. Bailey & R. MacDonald, eds.). Academic Press, London (335-417).
- MACLELLAN, H.E. & TREMBATH, L.T. (1991): The role of quartz crystallization in the development and preservation of igneous texture in granitic rocks: experimental evidence at 1 kbar. *Am. Mineral.* **76**, 1291-1305.
- MANNING, D.A.C. (1986): Contrasting styles of Sn-W mineralization in peninsular Thailand and SW England. *Miner. Deposita* **21**, 44-52.

- MARTIN, R.F. (1982): Quartz and the feldspars. In Granitic Pegmatites in Science and Industry (P. Cerný, ed.). *Mineral. Assoc. Can., Short-Course Handbook* 8, 41-62.
- NASKI, G.G. & HESS, P.C. (1985): SnO₂ solubility: experimental results in peraluminous and peralkaline high silica glasses. *Trans. Am. Geophys. Union* 66, 412 (abstr.).
- PARSONS, I. & BROWN, W.L. (1984): Feldspars and the thermal history of igneous rocks. In Feldspars and Feldspathoids (W.L. Brown, ed.). Reidel, Dordrecht, The Netherlands (317-371).
- PHILLIPS, E.R. (1974): Myrmekite - one hundred years later. *Lithos* 7, 181-194.
- PICHAVANT, M. (1987): Effects of B and H₂O on liquidus phase relations in the haplogranite system at 1 kbar. *Am. Mineral.* 72, 1056-1070.
- PRADITWAN, J. (1988): Mineralogy of tin and niobium-tantalum-bearing minerals in Thailand. In Tin Deposits in Asia and the Pacific (C.S. Hutchison, ed.). Springer-Verlag, New York (669-695).
- ROCKHOLD, J.R., NABELEK, P.I. & GLASCOCK, M.D. (1987): Origin of rhythmic layering in the Calamity Peak satellite pluton of the Harney Peak Granite, South Dakota: the role of boron. *Geochim. Cosmochim. Acta* 51, 487-496.
- SCHLIESTEDT, M. & JOHANNES, W. (1990): Cation exchange equilibria between plagioclase and aqueous chloride solution at 600 to 700°C and 2 to 5 kbar. *Eur. J. Mineral.* 2, 283-295.
- SECK, H.A. (1971): Der Einfluss des Drucks auf die Zusammensetzung koexistierender Alkalifeldspäte und Plagioklase im System NaAlSi₃O₈-KAlSi₃O₈-CaAl₂Si₂O₈-H₂O. *Contrib. Mineral. Petrol.* 31, 67-86.
- SILPALIT, M., MEESOOK, A. & LOVCHARASUPAPHON, S. (1985): Geological map sheet NC 47-3, Changwat Prachuap Khiri Khan (1:250,000). *Geol. Surv. Div., Dep. Mineral. Resources, Thailand.*
- SMITH, J.V. (1974): *Feldspar Minerals. 2. Chemical and Textural Properties.* Springer-Verlag, New York.
- STEMPROK, M. (1990): Solubility of tin, tungsten and molybdenum oxides in felsic magmas. *Miner. Deposita* 25, 205-212.
- TAYLOR, J.R.P. (1988): *Experimental Studies on Tin in Magmatic-Hydrothermal Systems.* Ph.D. thesis, Monash Univ., Melbourne, Victoria, Australia.
- _____ & WALL, V.J. (1992): The behaviour of tin in granitoid magmas. *Econ. Geol.* 87, 403-420.
- TAYLOR, R.G. (1979): *Geology of Tin Deposits.* Elsevier, Amsterdam, The Netherlands.
- TRUMBULL, R.B. (1991): Modelling the geochemical evolution of an Archean fertile granite-pegmatite. In Source, Transport and Deposition of Metals (M. Pagel & J.L. Leroy, eds.). Balkema, Rotterdam, The Netherlands (829-832).
- WALKER, R.J., HANSON, G.N., PAPIKE, J.J., O'NEIL, J.R. & LAUL, J.C. (1986): Internal evolution of the Tin Mountain pegmatite, Black Hills, South Dakota. *Am. Mineral.* 71, 440-459.

Received July 10, 1991, revised manuscript accepted September 15, 1992.